SIGET-#2
SIGAD-3

Technical Report No. 14

Contract N6 onr - 07129

NR 017 - 412

Physics of the Solid State

University of Illinois
Department of Physics
Urbana, Illinois

Principal Investigator

Robert J. Maurer

August 1954

U. S. Department of the Navy

Office of Naval Research

Washington, D. C.

SELF DIFFUSION IN SODIUM AND POTASSIUM CHLORIDE

Joseph Felix Aschner, Ph.D.
Department of Physics
University of Illinois
Urbana, Illinois

AD 43585

Bibliography of Technical Report No. 14, Contract N6onr-07129, NR 017-412.

This bibliography was omitted from the distributed copies of Technical Report No. 14.

Robert Maurer

Department of Physics
University of Illinois
Urbana, Illinois

October 27, 1954

Bibliography

(1) W. Lehfeldt, Z. Physik 85, 717 (1933)

(2) C. Tubandt, Handbuch der Experimental Physik Vol. XII/1, (1932)

(3) J. Frenkel, Z. Physik 35, 652 (1926)

(4) C. Wagner and W. Schottky, Z. Physik. Chemie B 11, 163 (1931)

(5) W. Schottky, Z. Physik. Chemie B 29, 335 (1935)

(6) W. Jost, Diffusion und Chemische Reaktion in festen Stoffen (Steinkopf, Dresden, 1937)

(7) N. F. Mott and M. J. Littleton, Trans. Faraday Soc. 34, 485 (1938)

(8) N. F. Mott and R. W. Gurney, Electronic Processes in Ionic crystals, (Oxford University Press, London, 1948) Ch II

(9) E. Koch and C. Wagner, Z. Physik. Chemie B 38, 295 (1937)

(10) W. J. Etzel and R. J. Maurer, J. Chem. Phys. 18, 1003 (1950)
ONR Technical Report No. 11, Contract N6ori-47, Task Order 2, 1949

(11) C. P. Bean, Thesis, University of Illinois, 1952 (unpublished)
C. P. Bean and R. J. Maurer, ONR Technical Report No. 4, Contract N6onr-07129, March 1952

(12) D. Mapother, H. N. Crooks, and R. J. Maurer, J. Chem. Phys. 18, 1231 (1950)
ONR Technical Report No. 8, Contract N6ori-47, Task Order 2, 1949
ONR Technical Report No. 12, Contract N6ori-47, Task Order 2, 1949

(13) H. Witt, Z. Physik 134, 117 (1953)

(14) A. Einstein, Ann. Physik (4) 17, 549 (1905)

(15) O. Stasiw and J. Teltow, Ann. Physik (6) 1, 261 (1947)

(16) J. Teltow, Ann. Physik 5, 71 (1949)

(17) J. W. Liddiard, Phys. Rev. 94, 29 (1954)

(18) E. Pitts, Proc. Roy. Soc. (London) A 217, 43 (1953)

(19) S. Kyropoulos, Z. anorg. allgem. Chemie 154, 308 (1926)

(20) I. Kolthoff and J. Lingane, Polarography (Interscience, N.Y. 1941)

(21) M. Born and J. Mayer, Z. Physik 75, [illegible] (1932)

(22) J. R. Reitz and J. L. Hummel, J. Chem. Phys. 19, 294 (1951)

(23) F. Bassani and F. G. Fumi, Nuovo Cimento 10, 274 (1954)

(24) F. Seitz, Rev. Mod. Phys. 18, 384 (1946)

(25) F. Seitz, Rev. Mod. Phys. 26, 7 (1954)

(26) I. Estermann, M. J. Leivo, and O. Stern, Phys. Rev. 75, 627 (1949)

(27) H. Hummel, Thesis, University of Goettingen, 1950

(28) H. J. Etzel, Phys. Rev. 87, 905 (1952)

(29) H. Kelting and H. Witt, Z. Physik 125, 697 (1949)

(30) F. Kerkhoff, Z. Physik 130, 449 (1951)

(31) G. J. Dienes, J. Chem. Phys. 16, 220 (1948)

TABLE OF CONTENTS

Acknowledgements

The author wishes to express his deep gratitude to Professor R. J. Maurer for suggesting this problem and for his guidance and encouragement throughout the course of the work.

The author also wishes to thank his many colleagues who helped him with the collecting of data during the strenuous days of working with the short-lived radioactive materials.

Special thanks are due Mrs. Marjorie Huse, who carried out many of the computations. The sponsorship of this project by the Office of Naval Research is gratefully acknowledged.

CHAPTER I

SELF DIFFUSION IN IMPURE SODIUM CHLORIDE

A. Introduction

Because of the simplicity of their crystallographic structure, the alkali halides occupy a prominent position in the field of solid state physics. X-ray diffraction experiments and all supplementary evidence indicate that an alkali halide such as sodium chloride has a cubic structure with sodium and chlorine ions so arranged that each sodium has six nearest neighbor chlorine ions and vice versa. A two dimensional representation of such a lattice is shown in Figure 1A.

The electrical conductivity of the alkali halides has been investigated by many workers, the pioneer work having been done by Lehfeldt[1] and Tubandt.[2] The latter also established the fact that the conductivity in alkali halides is ionic in nature. The observed conductivity can be explained by assuming the presence of imperfections in the lattice. This was shown by the theoretical investigations of Frenkel,[3] Wagner,[4] Schottky,[5] Jost,[6] and later Mott and Littleton.[7] Frenkel[3] proposed a defect in which a number of ions have been removed from their normal sites and displaced to interstitial positions in the lattice. This is shown in Figure 1B. Conduction can then take place by the motion of vacancies created when an ion is removed to an interstitial position, by the motion of interstitial ions, or by both. A different type of defect, illustrated in Figure 1C, has been proposed by Schottky.[5] It consists of

vacancies created in the lattice by the removal of an equal number of positive and negative ions from the interior to the surface of the crystal. Conduction in this case can take place either by the motion of positive or negative ion vacancies or both. The work of Schottky,[5] Jost,[6] and Mott and Littleton[7] has shown that the predominant defect in the alkali halides is of the Schottky type.

Both Frenkel and Schottky defects can be caused by thermal agitation, by the presence of impurity ions in the lattice, or by departure from exact stoichiometric proportions. Theoretical expressions for the concentration of these defects can be derived by minimizing the free energy.[8]

It was further observed by Lehfeldt,[1] and later by Koch and Wagner,[9] that when small amounts of a divalent salt were added to a monovalent alkali halide lattice the conductivity increased considerably. The mechanism causing this increase can be explained approximately in the following way. If a solid solution is formed in which a divalent positive ion replaces a monovalent positive ion in the lattice, then a second monovalent ion must leave the lattice to preserve electrical neutrality. Thus a positive ion vacancy is created for each divalent ion introduced substitutionally into the lattice. This situation is illustrated in Figure 1D. In recent years extensive studies of conductivity as a function of impurity content have been made by Etzel and Maurer[10] and by Bean and Maurer.[11]

Another process occurring in alkali halides which is

due to the presence of vacancies is that of diffusion. The ions in the crystal can diffuse from one part of the crystal to another by jumping into a vacancy, in turn leaving a vacancy behind. Self-diffusion of the cation has been measured by Mapother, Crooks, and Maurer[12] for NaCl and NaBr and by Witt[13] for KCl.

In view of the fact that the same mechanism is responsible for both conduction and diffusion, a relationship between the two exists. This was first derived by Einstein[14] (see also appendix I), and can be stated as

$$\frac{\sigma}{D} = \frac{ne^2}{kT} \qquad (1)$$

where

σ = conductivity

D = diffusion coefficient

n = density of carriers

e = charge of carriers

k = Boltzmann constant

T = absolute temperature.

This equation, however, is valid only if both conductivity and diffusion are brought about by exactly the same process, be it motion of the ions or motion of the vacancies. It should be pointed out that there are processes whereby diffusion can take place without the transport of electric charge, thus invalidating the Einstein relation. Such processes include the formation of positive ion vacancy-negative ion vacancy pairs (Figure 1E) and

divalent ion-vacancy complexes (Figure 1F). The reason such pairs and complexes invalidate the Einstein relation is due to the fact that they form neutral entities in the lattice. Thus the positive ion vacancy in each case will not contribute to the conductivity, but may contribute to the diffusion. (The contribution of the negative ion vacancy can usually be neglected, since its mobility is small compared to that of the positive ion vacancy).

The validity of the Einstein relation has been tested for NaCl and NaBr crystals by the work of Mapother, Crooks, and Maurer.[12] These investigators found the relation to be valid in the high temperature or intrinsic region (above approximately 500°C), but noticed a distinct deviation in the low temperature or structure sensitive region. The latter behavior they attributed to the existence of complexes, involving impurity ions present even in so-called "pure" crystals. In the intrinsic region, on the other hand, the thermally generated vacancies outnumber those introduced by impurities. Hence in this region the complexes become rather unimportant compared to the total number of vacancies, and the Einstein relation is satisfied.

The work of Etzel and Maurer[10] previously referred to also is concerned with these complexes. It was found that the addition of Cd^{++} ions to the NaCl lattice increased the conductivity, but not quite proportionately to the amount of Cd added. This was attributed to a larger number of complexes being formed per Cd^{++} ions added as the concentration is increased. From their results, Etzel and Maurer could obtain values for the

number of complexes formed per Cd^{++} ions added (or, as it is commonly referred to, the degree of association) for various concentrations and temperatures.

The purpose of the present experiment is to obtain a further check on the degree of association in the system NaCl NaCl + $CdCl_2$. This is achieved by measuring not only the conductivities of this system for various concentrations of Cd^{++} ions (and incidentally also over a wider temperature range than previous data), but also the self-diffusion coefficients of the Na^+ ion, using a radioactive tracer technique. The conductivity and the diffusion coefficients can then be compared by means of the Einstein relation. Any deviation should therefore yield direct information about the degree of association at that particular temperature and concentration. These results can then be compared with the theory.

B. Theory

In order to account quantitatively for the failure of the Einstein relation in some alkali halides with added divalent impurities, it is essential to know the number of complexes present as a function of temperature and impurity content, i.e. the degree of association. In addition, the binding energy of a complex must be obtained. We shall briefly derive the degree of association, using first a very simple approach and then a somewhat more detailed one. Then we shall show how the binding energy can be arrived at.

The basis of the calculations of the degree of

association is the mass action law. This approach was first used by Stasiw and Teltow,[15] later by Teltow,[16] Etzel and Maurer,[10] and recently by Lidiard.[17] The last two papers are of special interest in connection with the present work because they deal with the same system used here, i.e. $NaCl + CdCl_2$. We will follow in the main the paper by Lidiard, since it contains not only the relatively simple approach of the previous papers, but also considers the problem without some of the simplifying assumptions made by the earlier workers.

Let us take an alkali halide lattice containing N_+ solvent cations and N_i divalent impurity ions. At any given temperature let there be n complexes present, and hence N_i-n unassociated vacancies and N_i-n unassociated impurity ions. Then from the equilibrium condition

$$\text{unassociated impurity ion} + \text{unassociated vacancy} \rightleftharpoons \text{complex} \qquad (2)$$

the mass action law gives

$$\frac{N_+ n}{(N_i - n)^2} = K(T). \qquad (3)$$

It is to be noted that K(T) is independent of N_i, which has the significance of neglecting the mutual interactions between the unassociated vacancies and impurity ions. The effect of taking these interactions into account will be treated later.

An explicit form of K(T) is obtained by minimizing the free energy F_o with respect to n. Again neglecting the interactions of the unassociated charges, the free energy is given by

$$F_o = -kT \ln \frac{z^n \prod_{s=0}^{n} (N_+ + 2N_i - 2s)}{n!} \cdot \frac{(N_+ + 2(N_i - n))!}{N_+! (N_i - n)! (N_i - n)!} = \frac{ne^2}{\varepsilon r_o} \qquad (4)$$

The first term is the entropy term, z being the number of distinguishable orientations of a complex. (For the case of NaCl, the vacancy can be in 12 different nearest neighbor positions in the cation sublattice. Hence z = 12.) The second term represents the energy of association, ε being the static dielectric constant of pure NaCl, and r_o the nearest neighbor distance. (For the case of NaCl, $r_o = 2a$, where a is the anion-cation separation, and $\varepsilon = 5.62$).

Minimizing F_o with respect to n, we get

$$\frac{N_+ n}{(N_i - n)^2} = z \exp\left(\frac{e^2}{\varepsilon r_o kT}\right). \qquad (5)$$

The degree of association is defined by

$$p = \frac{n}{N_i} \qquad (6)$$

and can be obtained from (5). We thus find, using z = 12,

$$p = 1 - \frac{1}{y}\left(-1 + \sqrt{1 - 2y}\right) \qquad (7)$$

where

$$y = \exp\frac{T_o}{T} + \ln(24c) \qquad (8)$$

$$T_o = \frac{e^2}{\varepsilon r_c k} \qquad (9)$$

and

$$c = \frac{N_i}{N_+}. \qquad (10)$$

T_o as defined by (9) is the binding energy of a complex in units of Boltzmann's constant.

We next take into account the Coulomb interactions of the unassociated charges. This can be done by treating these charges as being equivalent to a solution of a binary electrolyte in a medium of dielectric constant ε. Such systems can then be handled by the Debye-Hueckel theory of electrolytes. This approach is legitimate even though the charges in question are in fixed lattice positions, rather than freely moving as in a true solution, since the average distance between these charges is much larger than the lattice spacing. Care must be taken, however, not to let unassociated vacancies and impurity ions approach closer than the next nearest neighbor distance. If they approached any closer they would then of course be classified as complexes.

The main effect of applying the Deby-Hueckel theory to the problem at hand is to introduce an additional term to the free energy, which must be taken into consideration when minimizing with respect to n. The details of this term as well as the new form that eq. (5) takes are contained in Lidiard's paper and will not be repeated here. We will merely quote the result for the NaCl type lattice with impurities, from which the degree of association can be calculated. It is

$$\frac{p}{(1-p)} = \exp\left[\frac{T_o}{T} + \ln(12c) - \frac{2(2\pi\sqrt{2})^{1/2}(T_o/T)^{3/2}\left[(1-p)c\right]^{1/2}}{\left\{1+4(\pi\sqrt{2})^{1/2}\left[(1-p)cT_o/T\right]^{1/2}\right\}}\right]. \qquad (11)$$

This equation can be solved for p by successive approximations. (See Lidiard's paper for details.)

Before we can apply equations (7) and (11) to compute the degree of association for specific impurity concentrations and temperatures, however, we still must determine T_o, i.e. the binding energy of a complex. There are at least three ways of doing this. Probably the simplest way is to take the Coulomb potential energy of two charges of opposite sign separated by a distance $\sqrt{2}a$, in a medium of dielectric constant ε. This gives

$$V = -\frac{e^2}{\varepsilon\sqrt{2}\,a} \tag{12}$$

from which we find $T_o = 7000^oK$, or a binding energy of .60 eV. In arriving at this value, however, we have completely neglected all interactions except the Coulomb interaction at the nearest neighbor distance. It will be shown below that these other interactions are by no means negligible.

A second way of finding T_o is due to Etzel and Maurer.[10] By writing the conductivity as

$$\sigma = \frac{2e^2\,\nu}{akT}\; e^{-U/kT}\; c(1-p) \tag{13}$$

where ν is the jump frequency of a vacancy and U the activation energy for such a jump, we find, substituting for p from (7), that

$$c = \alpha\sigma + 12e^{T_o/T}\,(\alpha\sigma)^2 \tag{14}$$

where

$$\alpha = \frac{akT}{2e^2\,\nu\; e^{-U/kT}}\,. \tag{15}$$

Etzel and Maurer then fitted their data of σ vs. c to a parabola

$$c = F\sigma + L\sigma^2\,. \tag{16}$$

By comparing (14) with (16), it is found that

$$12e^{T_o/T} = L/F^2 \tag{17}$$

from which T_o can be found. T_o turns out to be 3780°K, corresponding to a binding energy for the complex of .33 eV.

There are, however, some shortcomings in this method. First of all, we have neglected the effect of the atmosphere of unassociated impurity ions on the motion of the vacancies under the influence of a field. This effect will be a hindrance of the motion, thus σ must be multiplied by a factor (1-f), where $f<1$. An expression for f has been given by Pitts.[18] When applied to an NaCl type lattice, it results in the following equation for σ :

$$\sigma = \frac{2e^2\nu}{akT} e^{-U/kT} \quad c(1-p) \left\{ 1 - \right. \tag{18}$$

$$\left. \frac{2(2\pi\sqrt{2})^{1/2} c^{1/2} (1-p)^{1/2} (T_o/T)^{3/2}}{3(\sqrt{2}+1)\left[1+4(\pi\sqrt{2})^{1/2} c^{1/2}(1-p)^{1/2}(T_o/T)^{1/2}\right]\left[\sqrt{2}+4(\pi\sqrt{2})^{1/2} c^{1/2}(1-p)^{1/2}(T_o/T)^{1/2}\right]} \right\}$$

Secondly, in the previous method, the interaction between the unassociated charges have been neglected. This can be corrected by substituting into (18) the expression for p derived from (11). However, we then no longer find a simple relationship of the form (14). Specifically, a plot of $\frac{c}{\sigma}$ vs. σ gives a curve instead of a straight line. Thus the simple comparison between (14) and (16) can no longer be made.

The procedure now outlined was devised by Lidiard[17] to obtain a value for T_o without having to resort to the comparison mentioned above. From experimental data of conductivities measured as functions of impurity content and temperature $\frac{c+c_o}{\sigma}$ is plotted

against σ for various temperatures. Here c_o is the background impurity content, which is present even in the "pure" crystals. It must be added to c to avoid erroneous results for cases where $c \gg c_o$ does not hold. For each temperature selected, a smooth curve is then drawn through the plot of $\frac{c+c_o}{\sigma}$ vs. σ, and from these isotherms the values of σ for certain selected values of $c+c_o$ are taken. Since both T_o and $\nu e^{-U/kT}$ are unknown, the latter is eliminated by taking ratios $\frac{\sigma \text{ selected concentration}}{\sigma \text{ fixed concentration}}$ for all isotherms. The fixed concentration is the same for all these ratios, and the same selected concentrations are used for each isotherm. The only unknown in these ratios will be T/T_o. We thus can obtain sets of values T/T_o for each concentration, each value corresponding to one temperature. We next average T/T_o for each set, ending up with a value T/T_o for each temperature chosen. From this last set a mean value for T_o is then found. Using the data of Etzel and Maurer,[10] including a background impurity content of $c_o = .45 \times 10^{-5}$, corresponding to 10^{17} vacancies/cc, Lidiard obtained a value of 3900°K for T_o. This corresponds to a binding energy of .34 eV, very close to the value found by Etzel and Maurer.

We are now finally in a position to compute the degree of association, p, as a function of both the temperature and the concnetrations of impurity ions used in the present experiment. This is shown in Figures 6, 7, 8, and 9. Here p has been calculated on the basis of eq. (7) (dashed lines) and eq. (11) (full lines). It is shown that p falls off more rapidly with T when the Coulomb interactions are taken into account. This effect is the more pronounced the higher the impurity content. For the lowest impurity

content used the two curves of p virtually coincide. It should also be pointed out that while for very low temperatures p is unity, i.e. all vacancies are associated, this is well outside the region of experimentation, which extends from about 250°C to 700°C, or from $T/T_0 = .13$ to $T/T_0 = .25$.

C. Experimental Procedure:

The crystals used in this experiment were grown by means of the Kyropoulos,[19] technique. A platinum crucible of about 80 cm^3 capacity was filled with NaCl to which the proper amount of $CdCl_2 \cdot 2\ 1/2\ H_2O$ had been added. Both reagents were of the purest Baker and Adamson grade available. The crucible was then placed into a one kilowatt open ended Hoskins furnace and heated slightly past the melting point of NaCl (800°C). After all the salt had melted, a double-walled platinum tube with a small (about 3 mm x 3mm x 1 cm) NaCl seed crystal attached to its end was inserted into the melt for a few seconds and then withdrawn until the lower end of the seed crystal was just beginning to pull on the meniscus of the melt. As a result of this dipping procedure a layer of frozen salt was formed around the junction of the seed crystal and the platinum tube. This in turn provided both firm mechanical support and good thermal contact.

From this point on the procedure was to provide the proper thermal gradient to initiate and continue proper growth of the crystal. This was accomplished by means of passing compressed air through the platinum tube and slowly lowering the temperature of the furnace. Once growth had been initiated it was continued at an average rate of .15 mm/min. After about 3 mm were grown the

crystal was raised until its lower edge was again pulling on the meniscus. This procedure was repeated until a total length of 3 to 4 cm had been grown. Then the crystal was lifted clear out of the melt and allowed to cool down very slowly to room temperature.

The crystals so produced weighed from about 50 to 60 grams and used up about half the melt. It was also found empirically that the crystals tended to reject the Cd^{++} ions present in the melt. The ratio of the Cd added originally to the amount found in the crystal was about 8 to 1. This ratio was fairly constant throughout the entire range of concentrations used.

The diffusion measurements were performed in essentially the same manner as described by Mapother, Crooks, and Maurer.[12] The crystals grown as described above were annealed and then cleaved into specimens about 1 cm x 1 cm x 1/2 cm. A piece weighing about .1 gram, cleaved from the same crystal whose diffusion coefficient was to be measured, was bombarded by neutrons in the pile at the Argonne National Laboratory for about 24 hours. During this time the Na^{23} in the sample was activated to give Na^{24} (half-life 14.9 hours) to a sufficient extent to permit diffusion experiments to be carried on. Upon arrival at Urbana, the activity of the unshielded sample was generally found to be of the order of 10 mr/hr at 7 ft. By evaporation in high vacuum, a thin layer ($5-8 \times 10^{-4}$ cm) of radioactive NaCl was made to form on one surface of each specimen. In the earlier runs the specimens were then sealed off, two at a time, in evacuated pyrex capsules. For temperatures above 550° C the specimens were first inserted into a stainless steel container, to prevent the pyrex from collapsing

upon them. Later on this procedure was somewhat modified, as illustrated in Figure 2. The specimens (A) were first enclosed, again two at a time, in platinum capsules (B). The surfaces bearing the evaporated layer (C) of activated NaCl were set facing each other, kept separate by a thin platinum spacer (D). The platinum capsules were subsequently sealed off in vycor tubes (E) filled with helium gas. The helium for this purpose was passed through a liquid nitrogen trap before use. This served to freeze out most extraneous gases, the presence of which might contaminate the specimens. The pressure of the helium was such that at the diffusion temperature it would be approximately atmospheric. As a further precaution against contamination, the inside walls of the vycor tubes had been coated with a thin layer of NaCl (F). Such a layer was prepared by filling the tubes with chunks of NaCl and heating them to about 600°C under high vacuum, then cooling to room temperature.

From this point on, the procedure was the same regardless of whether the samples were enclosed in pyrex or vycor capsules. The capsule was placed in a stainless steel tube (Figure 2, (G)) which could be closed off at the bottom. The temperature could be measured by means of a chromel-alumel thermocouple (H). A correction of the order of 1°C proved necessary in the temperature reading since the thermocouple was not located inside the capsule. This correction was obtained by means of a dummy vycor capsule which was identical to the one shown in Figure 2, except that the specimens were not radioactive and had embedded in them a Pt-Pt Rh (10 %) thermocouple.

For the actual diffusion runs, the whole assembly shown in Figure 2 was placed in the center of a fused quartz tube running through a Hoskins furnace. The temperature of the furnace was controlled by means of a "Tag" celectray controller to within $\pm .4^{\circ}C$. The diffusion times were adjusted so that the product of the diffusion coefficient and the diffusion time was approximately 10^{-5} cm^2. However, no times shorter than 30 minutes were used, because the finite rise time and decay time of the temperature would then be too large a fraction of the total diffusion time. In order to make this fraction as small as possible, the sample was first put into a preheating furnace set at a much higher temperature for all diffusion runs under 2 hours. After reaching the desired diffusion temperature, the sample was then quickly transferred to the regular furnace. With a preheating furnace set at $1200^{\circ}C$ the samples could be heated from room temperature to $700^{\circ}C$ within 90 seconds. In addition to this lower limit on the diffusion time, an upper limit was imposed by the short halflife of the radioactive tracer. Thus it was found that no worthwhile diffusion measurements could be made for diffusion times exceeding 5 days, by which time the activity has decayed to 1/300 of its original value.

The slicing and counting procedure was identical to that described by Mapother, Crooks, and Maurer,[12] including use of the same microtome. The slices taken were 2 scale divisions (about 4.84×10^{-4} cm) thick and were collected on scotch tape. Most of the slices were counted until at least 10,000 counts had been recorded, so that the error due to the distribution of counts was held below 1 %. A number of corrections had to be applied, which

are listed as follows:

a) Dead time of counter (negligible below 40000 counts/min).

b) Background (17-19) counts/min).

c) Decay during the counting of one slice (negligible for counts less than 15 minutes in duration).

d) Decay during the counting of all the slices.

The corrected number of counts for each slice in a specimen was then plotted semilogarithmically against the square of the depth x. Unfortunately, the advance of the knife assembly downward was not uniform, so that x could not be taken as n times the thickness of one slice, where n is an integer. Through calibration with the interferometer mounted in the knife assembly of the microtome the exact depth at each slice was determined. Thus x was still taken as n times the thickness of one slice (set arbitrarily at 4.84×10^{-4} cm for all slices) but n now was no longer a set of integers, but depended on the vertical position of the knife. A typical semilogarithmic plot of counts I vs. n^2 is shown in Figure 5.

From the slope of such a plot as well as a knowledge of the diffusion time the diffusion coefficient can be determined. The equation (derived in appendix II) is as follows

$$D = \frac{1}{4t} \frac{n_a^2 - n_b^2}{\ln I_b - \ln I_a} \lambda^2 \qquad (19)$$

where

t = time of diffusion in seconds

I_a = activity in counts/min at point a

I_b = activity in counts/min at point b

n_a = depth in crystal at point a in units of one slice thickness

n_b = depth in crystal at point b in units of one slice thickness

λ = thickness of one slice in cm

D = diffusion coefficient in $cm^2/$

The errors involved in the diffusion coefficient arise from the following sources:

a) Errors in diffusion time. These errors are appreciable only for very short times and negligible for times longer than a few hours.

b) Errors in the slope, i.e. $\frac{n_a - n_b}{\ln I_b - \ln I_a}$. In most cases, these errors are only a few percent. However, for diffusion coefficients in the range of 10^{-12} to 10^{-13} cm^2/sec, where only a few countable slices can be taken, these errors become very large.

c) Errors in depth measurement. Such errors are due to the fact that $n\lambda$ does not represent exactly the depth of a slice. This is because of errors in the calibration and a slight change in calibration of the downward movement of the knife assembly when it moves through the same vertical range again. These errors are estimated to be about 2%, but will contribute a 4% error to D, because the depth appears as the square in eq.(19).

d) Errors arising from approximations made involving solution of the diffusion equation. This is discussed more fully in appendix II. At this point it may be stated, however, that these errors are mainly due to not using the exact solution of the diffusion equation and not taking into account the finite thickness of a slice. These errors are quite small for high diffusion coefficients but increase very rapidly for low ones.

e) Errors in temperature. It is believed that the temperature is known to within 1°C. This causes an error in D ranging from about 1 % in the high temperature region to 4 % at the lowest temperatures used in this experiment.

f) All other errors. They are believed not to exceed 1 %.

Since some of the errors depend directly or indirectly on the magnitude of the diffusion coefficient, we will list these errors in table I for various values of D.

Table I

$D(cm^2/sec)$	Source of error in D(%)						Total error in D(%)
	Time	Slope	Depth	Soln. of diffusion equation	Temp.	All other	
10^{-8}	5	2	4	3	1	1	16
10^{-9}	2	2	4	3	1	1	13
10^{-10}	1	2	4	3	1	1	12
10^{-11}	-	3	4	7	2	1	17
10^{-12}	-	15	4	12	3	1	35
10^{-13}	-	30	4	25	4	1	64

In general, then, we can say that the errors in the measured diffusion coefficient are about 15 % for all but very low values of D, and that for these values the accuracy of D diminishes very fast.

The conductivity was measured by a method similar to that used by Bean.[11] A sample was prepared by first cleaving a plate about 1 mm thick from a diffusion specimen prior to diffusion. Then both sides were painted with a suspension of graphite in alcohol, after which the actual sample (about 2 mm x 2mm) was

cleaved out. The sample was then placed between the two electrodes of a crystal holder. The original holder used in this experiment was identical to the one described by Bean, its main feature consisting of two 1 mil platinum electrodes spot-welded onto nickel buttons at the end of a thin-walled stainless steel tube. During the course of the experiment it was decided to modify this slightly to avoid possible contamination of the crystal due to the presence of nickel and stainless steel at high temperatures. The improved holder is shown in Figure 3. It consists of two solid platinum electrodes (A), one attached to the end of vycor tube (B), the other one moving freely inside another vycor tube (C), but held in place by 3 platinum wires (only 2 of which are shown in the Figure) and springs (D) in the cold temperature region. A Pt-Pt Rh(10%) thermocouple (E) is led in through two small Stupakoff seals. The platinum wires holding the lower electrode constitute the ground lead. The high lead consists of a platinum wire (F) running inside the inner vycor tube and being led out of the assembly by means of another Stupakoff seal (C) and an amphenol socket (H).

After a sample (I) had been put into place, the whole assembly was inserted into a vacuum tight quartz tube running through a Hoskins furnace and helium continuously circulated through the tube. The furnace temperature was regulated by a "Tag" celectray controller to within $\pm$ .2°C. Care was taken during each conductivity run to adhere as closely as possible to the same thermal cycle. This consisted of taking readings about 25 minutes apart at specified temperature intervals between 250°C and 700°C, the keeping the sample at 700°C for about 90 minutes, and then

taking readings at the same time and temperature intervals while the temperature was lowered again.

To measure the conductivity, an A.C. bridge technique was used. The circuit is illustrated schematically in Figure 4. The sample holder (C) is connected into one arm of a General Radio 716-C bridge. The generator is a Hewlett-Packard audio-oscillator (A), the null-meter a General Radio 736-A wave analyser (D). In addition, a General Radio 722-D precision condenser (E) has been put into the circuit for balancing purposes. Resistances from 10^{10} ohms down to 10^5 ohms were measured by a substitution method, balancing C_C and C_D with and without the sample in the circuit. The frequencies used ranged from 100 cycles/sec for the highest resistances to 10000 cycles/sec for the lowest ones, most of the readings being taken either at 1 kc or 10 kc. The accuracy of the resistance measurements is about 4 %, including a 1 % error in the frequency. For resistances lower than 10^5 ohms, an equal bridge arm technique was used. In this arrangement the upper arms of the bridge were adjusted to be equal and a Shallcross precision resistance box placed in parallel with the external balancing condenser. The value of the resistance needed for balance gives directly the parallel resistance of the sample and its holder. The resistance box was calibrated and found to be accurate to better than 1 %.

In computing the total errors in the conductivity, we must take into account two other sources of error in addition to the ones mentioned above. One of these is the uncertainty in the temperature, which causes errors in the conductivity ranging from 4 % at 250°C to 1 % at 700°C. The other source is a slight change

in the dimensions of the sample at high temperatures due to evaporation. This contributes at most a 2 % error, and can be neglected at low temperatures. We thus can state that the total error in the conductivity ranges from about 8 % at low temperatures (high resistances) down to 4 % at high temperatures. The conductivities are therefore known with much greater precision than the diffusion coefficients.

D. Results:

Four crystals of NaCl with varying concentrations of $CdCl_2$ were used in the conductivity and diffusion measurements. Various sections of these crystals were analyzed polarographically [20] for Cd content. In table II, the minimum, maximum and average molar ratios $\frac{Cd}{Na}$ are listed for these crystals. It should be pointed out that since some sections of the crystals were used more than once, both for conductivity and diffusion measurements, the average is weighted to reflect not only the concentration of each section but also the number of times it was used.

Table II

crystal	minimum $\frac{Cd}{Na} \times 10^5$	maximum $\frac{Cd}{Na} \times 10^5$	average $\frac{Cd}{Na} \times 10^5$
A	26	33	30
B	11	17	14
C	3	5	4
D	.4	.5	.5

The accuracy of the polarographic analysis ranges from about 25 % for the lowest concentration to 5 % for the highest.

Figure 10 shows the result of the conductivity measurements on the four crystals containing Cd (curves A, B, C, and D), and also, for comparison, the conductivity of a typical "pure" NaCl crystal (curve E). These data in each case represent an average taken from 4 to 6 different runs, some of which were taken on different sections of the crystal and some repeated on the same section. Each run was taken through the same thermal cycle, as outlined in the preceding section. A significant decrease has been

observed in the conductivity of crystals A, B, C, and D during the second half of the cycle. This decrease is the more pronounced the higher the concentration, ranging from about 8% for the lowest to 40 % for the highest. No such decrease has been observed for "pure" NaCl crystals or crystals containing Ca[11] instead of Cd. Similar observations have also been made by Etzel and Maurer.[10] The evidence based on their as well as the recent work is far from conclusive. However, it appears that both a volume and an electrode-crystal interface effect are present. In the former, Cd^{++} ions are somehow removed from the volume of the crystal, perhaps to form larger aggregates. This would effectively cut down the number of vacancies and hence the conductivity. As far as the second effect is concerned, it is believed that some form of a high-resistance layer is formed at the interface between the crystal and the graphite electrode. It is not clear why this should occur when Cd^{++} ions are present and not when we are dealing with the same experimental arrangement but with Ca^{++} ions present or else no deliberately added impurity. The whole problem needs to be investigated in greater detail. It can be stated, however, that on the basis of the present evidence it appears that the volume effect outweighs any other effect.

Figures 11, 12, 13, and 14 show the diffusion coefficients measured by means of radioactive tracer methods. On the same plot the diffusion coefficients calculated from the measured conductivities by means of the Einstein relation are shown (full lines). The conductivities used for this purpose are the ones shown in the lower half of each cycle in Figure 10. We have also calculated the diffusion coefficients based on what the conductivities would

be were there no association. The relation used was

$$\sigma_{\text{measured}} = (1-p)\,\sigma_{\text{no association}} \qquad (20)$$

This is also shown in Figures 11, 12, 13, and 14. The dotted lines correspond to p calculated from (7), and the dashed lines to p calculated from (11). In Figure 14 these two lines are so close together as to virtually coincide.

As expected, the curves based on $\sigma_{\text{no association}}$ lie higher than the ones based on σ_{measured}. Further, since p determined from (7) is greater than p determined from (11), the values of D calculated based on the simple theory of association are larger than those based on the more detailed theory. It can also be noted from these Figures that the effect of taking p into account increases with concentration and decreases with temperature.

The failure or satisfaction of the Einstein relation and the conclusions that can be drawn from it will be discussed in the next section. We will limit ourselves at this point to some remarks on the scattering of the measured diffusion coefficients. As already pointed out in the preceding section, the diffusion coefficients obtained by radioactive tracer techniques are subject to much greater errors than the conductivity measurements. In addition to these errors, the spread in concentration of impurity over a crystal, in view of the relatively large size of the diffusion specimens, causes errors of up to 20 %, which is of about the same order as all the other errors combined. An attempt has been made to minimize these additional errors by cleaving the specimens from as small a section of the crystal as possible, and by using them over again two or three times at different temperatures. Nevertheless, in

view of the large errors and the small number of points involved, as compared to conductivity measurements, an averaging process is probably meaningless and has been omitted here. The scattering of the measured diffusion coefficients shown in Figures 11, 12, 13, and 14 is, with one or two exceptions, well within the range of experimental error. Where measurements on two specimens at the same temperature were made, the larger diffusion coefficients usually corresponds to a specimen with a slightly higher Cd content. But even here, in a few instances, the order is reversed, indicating that the other errors, discussed in the previous section, are also appreciable. It should be pointed out, however, that there is less scattering of diffusion data in the present work than has been found in the intrinsic region of "pure" salts, such as KCl,[13] NaCl,[12] and NaBr,[12] even though presumably there were no concentration gradients in these "pure" crystals.

E. Discussion:

We first consider the conductivities shown in Figure 10. In the low temperature region (below about 400°C) they follow more or less straight and parallel lines. The slope is given by $-U/kT$, where U is the activation energy for the jump of a vacancy. The value of U obtained from the present data is .85 eV, the same as was found by Etzel and Maurer.[10]

This very uniform behavior of the conductivities in the low temperature region can easily be explained by the fact that we are entirely in the structure sensitive region. This means that almost all of the vacancies contributing to the conductivity are those introduced by impurities. Hence the energy of creation of a vacancy

does not enter into the expression for the conductivity. Strictly speaking, there is a temperature dependence in the pre-exponential factor of the conductivity, i.e.

$$\sigma = \frac{A}{T} \quad e^{-U/kT} \tag{21}$$

However, the change in σ with T in the low temperature region is almost entirely due to the exponent.

In the high temperature region the conductivities curve upward, as expected, since now the thermally generated vacancies begin to equal and eventually outnumber the impurity vacancies. Thus we can write

$$\sigma = \frac{A}{T} \quad e^{\frac{-U+W/2}{kT}} \tag{22}$$

where W is the energy necessary to create a vacancy pair. It is further apparent from Figure 10 that the lower the impurity concentration, the lower the temperature at which the upward curving of the conductivities begins.

This simple treatment, however, fails to explain why the slopes are not constant until the thermal vacancies begin to contribute. At temperatures well below the ones where this contribution appears there is a distinct downward curving of the conductivities, as can be seen from Figure 10. A possible explanation of this phenomenon has been suggested by Bean.[11] According to his theory, the jump frequency of a vacancy will be affected by the vibrations of the two negative ions that stand in the way, since it is easier for the vacancy to jump when the two negative ions are moving away from each other. Thus the pre-exponential factor in (21) is changed. According to Bean, the result is

$$\sigma = \frac{A'}{T^3} e^{-U/kT} \qquad (23)$$

The present data are indeed fitted better by (23) than by (21), but the fit is by no means perfect. A good fit would result from $T^{5/2}$ in the denominator of (23) instead of T^3. Thus other factors must be operating in the system NaCl + $CdCl_2$ for which at present there is no simple explanation.

Before passing to a comparison of the measured and calculated diffusion coefficients shown in Figures 11, 12, 13, and 14, let us first consider some of the assumptions involved. The first assumption made is that the same volume effect which causes a decrease in the conductivity also causes a decrease in the diffusion. Since both are based on a vacancy mechanism and since the net result of the volume effect is to cut down the number of vacancies, such an assumption seems reasonable. It is for this reason that in comparing the measured and calculated diffusion coefficients the lower half of the conductivity in each cycle was used. The probable correctness of this assumption is further emphasized by the fact that using it the Einstein relation is satisfied in the high temperature region, whereas using the higher values of σ (upper half of cycle), $D_{calculated}$ would lie well above $D_{measured}$. Now there have been a number of mechanisms proposed which would cause $D_{calculated}$ to lie below $D_{measured}$, but none that would permit the opposite. Indeed, previous work on self-diffusion in "pure" alkali halides [12,13] has always either resulted in the Einstein relation being satisfied or else some mechanism has been proposed which would permit some vacancies to contribute to diffusion but not to conductivity.

The second assumption concerns the effect of the atmosphere of impurity ions in hindering the motion of vacancies (see eq. (18)). If one fixes a point of reference inside a crystal, most of the motion of the vacancies past this point under the influence of a field would appear to be a random jumping rather than drift. In the steady state, however, a definite displacement of the vacancies with respect to the impurity ions will have occurred under the influence of a field, while it would not be reasonable to assume that such a displacement occurs when no field is present. Thus the retardation effect is present in the conductivity and not in the diffusion. Therefore in applying the Einstein relation $D_{calculated}$ should be corrected by the factor (1-f) while $D_{measured}$ should not. This has been neglected here, because the correction even for the highest impurity concentration would only be a few percent, and quite negligible for lower concentrations. For a much higher concentration of impurity, on the other hand, such as can be achieved with Ca and perhaps other metals, though not Cd, this effect could not be neglected.

The third assumption concerns the binding energy of a complex, which we have taken to be .34 eV. This value was arrived at by fixing both the binding energy of a complex and the magnitude of the interactions at large distances. This is obviously a much better value than the one obtained from eq. (12), i.e. .60 eV, completely neglecting these long-range interactions. Furthermore, using $T_o = 7000°K$ in eq. (7) or eq. (11) would give degrees of association at or near 100 % for most of the crystals used in the present work, an obviously absurd conclusion. However, by taking .34 eV as the real binding energy of a complex, we underestimate

somewhat the effect of the long-range interactions. This in turn results in overestimating the degree of association calculated by eq. (11). In order to apply the theory correctly it is necessary to take into account the non-Coulombic interactions between the vacancies and the impurity ions, both at nearest neighbor separations and at larger distances. These interactions are due to the repulsive energy, distortion of the lattice around a defect, and polarization due to dipoles created by displacement of ions and electronic polarizability. They have been considered previously by Born and Meyer,[21] Mott and Littleton,[7] and Reitz and Gammel.[22] The latter obtained a binding energy for the Cd^{++} ion-vacancy complex in NaCl of .44 eV, which is almost the same as the Coulomb interaction energy of an impurity ion and a vacancy in next nearest neighbor positions (.43 eV). A very recent computation by Bassani and Fumi[23] contains some improvements over the work of Reitz and Gammel. Their result for the binding energy of the complex in question is .38 eV and may be considered to the the best present theoretical value. Bassani and Fumi did consider non-Coulombic interactions as far away as next nearest neighbor positions. Now Lidiard[17] points out that it does not make much difference in connection with our problem whether we take the limiting distance differentiating between complexes and unassociated charges to be twice the lattice constant or ten times the lattice constant. If we can therefore assume that non-Coulombic terms are of little importance past the next-nearest neighbor separation, to apply the theory correctly we need only use .38 eV instead of .34 eV for the binding energy and assume the limiting distance of association to be the next-nearest neighbor distance. This would result in p

increasing slightly at any given temperature, regardless of whether eq. (7) or eq. (11) is used. The only correction still necessary to the theory of association would now be the non-Coulombic interactions at larger than next-nearest neighbor positions. These are presumed to be quite small.

The main result of our assumption regarding the binding energy is then that a small correction may be necessary which would shift the curves of $D_{calculated}$ based on either eq. (7) or eq. (11) slightly upward. It would not, however, materially affect any of the conclusions reached as a result of this work.

We are now in a position to discuss the main part of the present work, that is, the failure or satisfaction of the Einstein relation as a function of concentration and temperature and the conclusions that can be drawn there from regarding the degree of association. From the results shown in Figures 11, 12, 13, and 14 it is apparent that the Einstein relation is satisfied for all concentrations in the high temperature region. However, since the degree of association even for the highest concentration is only about 10% at these temperatures, it is impossible to say, in view of the large error in $D_{measured}$, whether the Einstein relation holds on the basis of $\sigma_{measured}$ or $\sigma_{no\ association}$. In the low temperature region, however, both crystals A and B show a significant deviation from the Einstein relation if we use $\sigma_{measured}$ as a basis. This deviation is well outside the limit of experimental error. This is believed to be definite evidence that there is a considerable degree of association in these crystals in the low temperature region. When we compare $D_{measured}$ against $D_{calculated}$ on the basis of eq. (7) and eq. (11), we find that for crystal A

eq. (7) represents the degree of association somewhat better than eq. (11). In crystal B the evidence is much less conclusive, especially since the curves representing $D_{calculated}$ on the basis of the two equations lie closer together. There the errors in $D_{measured}$ are of the same order as the difference between these two curves. However there is no question that a significant degree of association also is present in crystal B.

In crystals C and D no deviation from the Einstein relation can be found. But here $D_{calculated}$ on the basis of $\sigma_{measured}$ or either form of $\sigma_{no\ association}$ lies within the range of probable error of $D_{measured}$, so this behavior is understandable. There is, however, a significant point that must be brought up here in this connection. The work of Mapother, Crooks, and Maurer[12] has shown that a significant deviation from the Einstein relation occurs in "pure" NaCl and NaBr in the low temperature region. This deviation correpsonds to a degree of association of about 50%. It is believed that this very large degree of association is due to one or more types of impurity ions in the background impurity content, which, in contrast to Cd, are very highly associated. Spectrographic analysis of "pure" NaCl shows at least 25 impurity elements present. Of these Fe, Mn, Mg, As, Sn, Sb, Hg, Pb, Cu, Zn, Ni, Co, Ba, Ca, Cr, Al, Zr, and Ti are possible candidates for such an effect. Let us now on the other hand consider crystal D. The measured conductivity is about six times and the measured diffusion coefficient three times that of Mapother's "pure" NaCl crystals. In a crystal containing $2N_i$ Cd ions we would thus have N_i of these highly associated background impurity ions to obtain the same ratios for the diffusion coefficients. But while the $2N_i$ Cd atoms would

contribute equally to the conductivity (the degree of association being negligible) only half the N_i background impurity ions would contribute, assuming a 50% degree of association. Thus for crystal D we would expect $\frac{D_{measured}}{D_{calculated}} = \frac{3}{2\ 1/2} = \frac{1}{1-p}$. Hence p = 1/6 or 16.6%. This would certainly not cause a deviation beyond the limit of error in $D_{measured}$ for the very low diffusion coefficients in crystal D, and therefore it is not surprising that the effect of the background impurities cannot be detected. This illustration, however, serves to show that for higher concentrations of Cd the effect of the background impurities will be completely masked.

In summary, then, we may say that a deviation from the Einstein relation can be detected in those crystals where it is large enough to be beyond the range of the experimental error in $D_{measured}$. This deviation is approximately that expected on the basis of the theory of association. However, it is not possible to state conclusively whether the present data are fitted better by the simple theory of association (eq. (7)) or by the more detailed theory resulting in eq. (11).

In conclusion, it might be of value to suggest a few related experiments which might shed further light on the subject of association. This would also include improving the present experiment by producing a more uniform Cd^{++} ion concentration (higher $\frac{melt}{crystal}$ ratio) and if possible also crystals of higher Cd content. The former would cut down the error in $D_{measured}$, and the latter would produce a greater degree of association, which might be checked more quantitatively. Next, a different divalent ion, like Ca^{++} or Sr^{++}, and a different solvent salt, like KCl, might be used. Crystals of a molar ratio Ca/Na up to 25×10^{-4} have been grown by

Bean.[11] Since according to Bassani and Fumi [23] the Ca, Cd, and Sr complexes in both NaCl and KCl have approximately the same binding energy (all lie between .32 eV and .45 eV), we would expect very large degrees of association for high impurity content. Thus, it may be possible to decide quantitatively whether eq. (7) or eq. (11) better describes the degree of association. In addition, the system NaCl + $CaCl_2$ has the advantage of not having the annoying decrease of conductivity with time. Going now to pure crystals, the theory that highly associated background impurity ions are responsible for the results of Mapother, Crooks, and Maurer,[12] could be checked by producing "pure" crystals (possibly by zone melting) that have one or two orders of magnitude less impurity content than the usual "pure" crystals (10^{17} vacancies/co). There should be much less association in such very pure crystals. The disadvantage of having very low diffusion coefficients with a consequently large probable error may make this experiment difficult, however.

Finally, the diffusion coefficient of a divalent impurity ion may be measured directly by using an isotope of this ion as a tracer. If a large degree of association exists, then such an ion, having so to speak a built-in vacancy into which it can jump, should have an exceedingly high diffusion coefficient. The difficulty here lies in activating the relatively few impurity ions in the lattice to a sufficient extent to carry out the tracer technique. Such an experiment has failed for this reason with the system NaCl + $CdCl_2$. It may succeed with the system NaCl - $CaCl_2$, since 10 times more Ca than Cd can be built substitutionally into the lattice. Also, the slow-neutron cross-section of Ca is considerably

higher than that of Cd for the isotope suitable for a diffusion experiment. Success of such an experiment might be insured by making use of a neutron flux higher than is now available either at Oak Ridge or at the Argonne National Laboratory.

CHAPTER II

SELF DIFFUSION IN PURE POTASSIUM CHLORIDE

A. Introduction:

While the work described in Chapter I was in progress, H. Witt of the University of Goettingen published data[13] on the temperature dependence of the self diffusion coefficient of the potassium ion in potassium chloride. In the neighborhood of 600°C, where the vacancy content of the crystals should be uninfluenced by impurities, Witt found a deviation from the Einstein relation between diffusion coefficient and electrical conductivity. This behavior of KCl is unlike that of NaCl and NaBr as determined by the work of Mapother, Crooks, and Maurer.[12] As already indicated in the previous chapter, at temperatures sufficiently high that the accidental impurities had no effect upon the vacancy concentration, these investigators found the Einstein relation to be satisfied in NaCl and NaBr.

The present work was undertaken to check the data of Witt since his results had rather interesting implications. In particular, Witt's data furnish evidence for the existence of pairs of positive and negative ion vacancies in KCl. Such pairs are illustrated in Figure 1F. The mechanism by which pairs may account for failure of the Einstein relation has already been discussed (see p.3).

There is some additional evidence suggesting although not conclusively establishing the existence of pairs. Seitz[24,25] has proposed that pairs may be responsible for the relatively rapid migration of color centers in KCl, as observed by Estermann, Leivo, and Stern,[26] and for the enhanced darkening of X-ray colored KCl

and NaCl with additive $CaCl_2$.[27,28] Also, the formation of pairs is favored by the fact, pointed out by Seitz,[25] that there is no energy minimum for the configuration of vacancies of opposite sign in next-nearest neighbor positions. This means that such vacancies will automatically be drawn together to form a pair when they approach as closely as the next-nearest neighbor distance.

In view of all these facts it was therefore deemed advisable to determine as accurately as possible whether pairs contribute appreciably to the self diffusion coefficient of the cation in KCl. While a negative answer would not rule out the existence of pairs, an affirmative result would make more plausible the explanation of other phenomena in terms of the pair hypothesis.

B. Experimental Procedure:

With a few modifications, the experimental procedure for KCl was the same as that described for NaCl in the previous chapter. No crystals were grown for this part of the experiment, however, but instead large single crystals of KCl were obtained from the Harshaw Chemical Company, which were then annealed and cleaved much like the NaCl crystals. Neutron irradiation was again performed at the Argonne National Laboratory. However, since the relative abundance of the potassium isotope which was activated, namely K^{41}, is less than 7 % (as compared to 100 % for Na^{23}), the activities of the activated KCl were considerably smaller than those for NaCl. Upon arrival at Urbana, the average activity of the unshielded KCl was about 10 mr/hr at 4 feet. This fact and also the shorter half-life of K^{42} (12.44 hours) placed an upper limit of about 3 days on the diffusion time. As a consequence, no diffusion measurements

could be made below 500°C.

The method for sealing off the diffusion specimens was identical to the modified procedure described in Chapter I (pp. 13 and 14) and illustrated in Figure 2. In contrast to NaCl, however, it was found that at high temperatures the KCl crystals were exceedingly sensitive to contamination. This effect was in the form of a pink layer extending some distance into the crystal from all sides. It was especially pronounced in preliminary experiments where stainless steel capsules were used, but could also be observed when the specimens were merely sealed in vycor which had not been coated with KCl on the inside. The KCl coating, the helium, and the platinum capsules inhibit the reaction between the specimens used and the vycor. With all these precautions, no coloring of the crystals could be observed even when left at high temperatures for extended periods of time. On the basis of these facts it is believed that a metal diffuses into the KCl crystals at high temperatures. It has also been noted that the pink crystals exhibited considerably higher self diffusion coefficients than the clear ones. This is expected if di- or tri-valent metallic impurity ions have diffused into the lattice, lending further strength to the belief that the pink color is due to such ions.

Still another consequence of the KCl coating of the vycor is the fact that the samples retained the fresh, clear appearance of newly cleaved surfaces. Samples diffused without this coating had grayish, dingy looking surfaces, and in particular the evaporated layer of KCl became greyish yellow in color. Possibly this is due to some organic matter adhering to the vycor. The liquid

nitrogen trap also helps in this respect, perhaps freezing out organic vapors present in the system.

The slicing of the KCl specimens was carried out in the same manner as NaCl. However, it was found that the softer KCl was not removed as uniformly by the microtome knife as NaCl, leading to considerable scattering of data on the log activity vs. $(\text{depth})^2$ curves. If the knife orientation across the crystal surface was along the 110 direction the KCl came off in long needles rather than in powder form, and effective slicing was almost impossible. But even with the knife oriented in a different direction the slices had to be taken 50 percent thicker than for NaCl. Otherwise there was danger of the scotch tape contacting the knife.

The errors in the diffusion coefficients are somewhat larger than for the case of NaCl, the reason being primarily the increased thickness of the slices. This has the effect that fewer slices can be taken (hence larger error in slope) and greater approximations have to be made when solving the diffusion equation. It is estimated that the errors range from 20 % at 700°C to 40 % at 500°C. However, these errors do not appear sufficient to account for the scatter of the data shown in Figure 18. It is not known at the present time why KCl data are inferior in precision to NaCl data which are taken by the same personnel using the same equipment.

The conductivity also was measured by the same methods discussed in Chapter I. There was no change in conductivity in the intrinsic region during any cycling process. In the structure sensitive region, however, the conductivity increased considerably during the second half of a cycle. This effect is attributed to

contamination of the sample. It was much reduced when the improved sample holder shown in Figure 3 was put into operation. The precision of the conductivity measurements is the same as for NaCl. However, since there was no volume effect and no concentration gradient, successive measurements on different samples in the intrinsic region were within a few percent of one another.

C. Results and Discussion:

The conductivity measurements made on four different specimens are shown in Figure 17. The specimens are not distinguished in this graph because of the uniformity of behavior, slight deviations occurring only below 400°C. The "knee" of the curve is located near 450°C. This gives an indication of the purity of the crystals. The concentration of vacancies due to impurity ions is of the order of 2×10^{15}/cc. This number has been obtained by taking the data of Kelting and Witt[29] (who plotted the concentration of thermal vacancies vs. temperature) and by assuming that at the "knee" the concentration of thermal vacancies is equal to the concentration of impurity vacancies. Harshaw NaCl crystals used in previous work have been found to contain an impurity vacancy content of 10^{17}/cc, so that the crystals used in the present work are appreciably purer.

Figure 18 shows the results of eighteen diffusion experiments covering the temperature range from 520°C to 660°C. The solid curve represents the diffusion coefficient calculated from the conductivity by means of the Einstein relation. Since the contribution of the chloride ion to the conductivity is appreciable

in KCl at high temperatures, the transference number data of Kerkhoff[30] were used to obtain the contribution due to the potassium ion alone.

In view of this contribution of the chloride ion, we must use only the conductivity σ_+ due to the K^+ ion in the Einstein relation. The total conductivity σ (shown in Figure 17) is related to σ_+ by

$$t_+ = \frac{\sigma_+}{\sigma} \qquad (24)$$

where t_+ is the transference number of the K^+ ion. For temperatures in excess of 620°C the calculated diffusion coefficient is represented by a dashed line since it was necessary to extrapolate Kerkhoff's data above this temperature.

From the slope of the line in Figure 18 we can get the sum of the activation energy, U, and the energy of formation, $\frac{W}{2}$, of a single positive ion vacancy. Unfortunately, neither U nor $\frac{W}{2}$ are known separately with great accuracy. Using the value of 1.20 eV for $\frac{W}{2}$ from Kelting and Witt[29] and 1.88 eV for $U + \frac{W}{2}$ from the present work, we find U to be .68 eV.

In this connection it might be of interest to mention briefly a calculation by Dienes,[31] who obtained a theoretical value for the activation energy for the jump of a pair in KCl. In order that a neutral pair may diffuse it is necessary that ions of both charges jump into the corresponding vacancies. Since the negative ion is much less mobile than the positive one, the rate-determining step must be the migration of the negative ion. Now the missing positive ion lowers the barrier opposing the movement

of the negative ion vacancy, hence there is a drop in activation energy of a pair as compared to that of a single negative ion vacancy. Using the method of Born and Mayer[21] as modified by Mott and Littleton,[7] Dienes arrived at an activation energy for the pair of .375 eV. This value may be somewhat in error, but it seems likely that the activation energy does not exceed .5 eV. It is thus considerably below that for a single positive ion vacancy.

It therefore appears that pairs may have rather large mobilities. However, the results presented in Figure 18 show that the Einstein relation is satisfied for KCl in the temperature range covered by these experiments. Thus even if the mobility of the pairs should be large, their concentration is probably not sufficient to enable them to contribute appreciably to the diffusion.

The data of Witt[13] are also shown in Figure 18. The present data do not agree with those of Witt. We believe Witt's results to be affected by an unknown constant error.

In conclusion we may say that the present data lend no support to the theory that vacancy pairs exist in KCl in the intrinsic region. While the existence of such pairs is not ruled out, either their mobility or more probably their concentration (or both) are too small to influence the self diffusion coefficient of the potassium ion.

APPENDIX I

THE EINSTEIN RELATION

We shall derive the Einstein relation first by a general thermodynamic argument and then from an atomistic point of view with special reference to diffusion and conduction as they are supposed to occur in alkali halide crystals. Since the experimentally measured diffusion and conduction are essentially one-dimensional, we shall limit our derivations to the one-dimensional case.

Let us suppose we have particles of charge e in an electric field $E = -\frac{\delta\varphi}{\delta x}$. Then the density of particles at a point x is given by Boltzmann's equation as

$$n(x) = \text{const } e^{-e\varphi/kT} . \tag{25}$$

The current density of charged particles under the influence of the field can be expressed by

$$i = neuE = -neu \frac{\delta\varphi}{\delta x} \tag{26}$$

where u is the mobility. This current flow will create a concentration gradient, and thus give rise to a diffusion current opposing the buildup of this concentration gradient. The diffusion current density is given by

$$i = -e\ D \frac{\delta n}{\delta x} \tag{27}$$

where D is the diffusion coefficient. In the stationary state no current is flowing, and we have

$$-neu \frac{\delta\varphi}{\delta x} - e\ D \frac{\delta n}{\delta x} = 0 \tag{28}$$

By integrating (28) we obtain immediately

$$n = \text{const } e^{-\frac{eu\varphi}{D}} . \tag{29}$$

Comparing (25) and (29), we arrive at

$$\frac{u}{D} = \frac{e}{kT} \tag{30}$$

which is the form the Einstein relation is often given. To obtain the form used in the present work, we substitute $\sigma = neu$ in (30). We thus obtain

$$\frac{\sigma}{D} = \frac{ne^2}{kT} \tag{31}$$

which is identical to (1).

Next let us consider a more detailed model consisting of an atomic lattice in which the atoms are separated from their nearest neighbors by a distance a. The atoms in their equilibrium positions lie in energy troughs of height U. The probability per second of an atom making a jump into a neighboring position in the absence of a field is given by

$$p = \frac{v}{3} \frac{n_v}{n} e^{-U/kT} . \tag{32}$$

In this expression $e^{-U/kT}$ is the probability that the atom has enough energy to overcome the barrier, v is the vibration frequency of the atom, $\frac{1}{3}$ is the probability that the atoms will be vibrating in the x direction, and $\frac{n_v}{n}$ gives the probability that the adjoining lattice site will be vacant. Here n_v is the density of vacancies and n the density of atoms.

Now let us assume that a concentration gradient exists (e.g. some of the atoms are radioactive). The flux P of such "tagged" atoms across a plane A normal to the x direction and midway between

two atomic planes is given by the flux of such atoms jumping across it from one direction minus the flux of such atoms jumping the opposite way. Each flux is given by the number of tagged atoms per cm^2 on the atomic plane adjoining the fictitious plane A times the jump probability per second across the plane. Hence

$$P = an_1^* p_{12} - an_2^* p_{21} \tag{33}$$

where n_1^* and n_2^* are the densities of tagged atoms on either side of plane A, and p_{12} and p_{21} are the respective jump probabilities per second. In the absence of a field, $p_{12} = p_{21} = p$. However, due to the concentration gradient $n_1^* \neq n_2^*$. Substituting (32) in (33) we obtain

$$P = a^2 \frac{n_1^* - n_2^*}{a} \frac{n_v}{n} \frac{\nu}{3} e^{-U/kT} = -a^2 \text{grad } n^* \frac{n_v}{n} \frac{\nu}{3} e^{-U/kT} . \tag{34}$$

Using the definition of the diffusion coefficient

$$P = -D \text{ grad } n^* \tag{35}$$

we get

$$D = a^2 \frac{n_v}{n} \frac{\nu}{3} e^{-U/kT} . \tag{36}$$

The conductivity may be derived in a similar manner. Suppose a uniform field E exists in the x direction. The current density across plane A can now be written as

$$i = eP = ean_1^* p_{12} - ean_2^* p_{21} . \tag{37}$$

We are no longer concerned with tagged atoms, since both tagged and untagged atoms have the same charge e. Thus $n_1^* = n_2^* = n$. However, the field E alters the height of the barrier, increasing

it by $\frac{eEa}{2}$ in one direction and decreasing it by the same amount in the opposite direction. Hence $p_{12} \neq p_{21}$. The new jump probabilities per second will be

$$p_{12} = \frac{n_v}{n} \frac{\nu}{3} e^{-(U/kT - \frac{eEa}{2kT})} \tag{38}$$

and

$$p_{21} = \frac{n_v}{n} \frac{\nu}{3} e^{-(U/kT + \frac{eEa}{2kT})} \tag{39}$$

Substituting (38) and (39) into (37), we obtain

$$i = e a n_v \frac{\nu}{3} 2 \sinh \frac{eEa}{2kT} e^{-U/kT} \tag{40}$$

Under normal laboratory conditions $eEa \ll skT$, so the hyperbolic sine may be replaced by its argument. We then have

$$i = \frac{e^2 a^2 n_v \nu}{3kT} e^{-U/kT} E \tag{41}$$

Using the definition for conductivity

$$i = \sigma E \tag{42}$$

we thus get

$$\sigma = \frac{e^2 a^2 n_v \nu}{3kT} e^{-U/kT} \tag{43}$$

Comparing (36) and (43), we again arrive at (31).

APPENDIX II

THE DIFFUSION EQUATION AND ITS SOLUTION

The basic law for one-dimensional diffusion of particles is known as Fick's first law and can be stated as

$$P = - D \frac{\delta I}{\delta x} . \qquad (44)$$

P is the flux of particles (number crossing unit area perpendicular to the x direction per unit time), D is the diffusion coefficient, and I is the density of particles. (We choose the symbol I because it represents the radioactivity which is our measure of the density of the particles as it applies to this experiment.)

Equation (44) holds for the stationary state. From it we can derive another law which will apply to the non-stationary state. Let us consider two planes of unit area at positions x and x+dx and perpendicular to the concentration gradient $\frac{\delta I}{\delta x}$. We can write the accumulation of particles between the planes as $P - P + \frac{\delta P}{\delta x} dx$ or $-(\frac{\delta P}{\delta x})dx$. As a result, the concentration increases, and we can also write the accumulation between the two planes as $(\frac{\delta I}{\delta t})dx$. Equating the two, we get

$$-(\frac{\delta P}{\delta x}) = \frac{\delta I}{\delta t} . \qquad (45)$$

If D is independent of the concentration, (44) and (45) yield

$$D \frac{\delta^2 I}{\delta x^2} = \frac{\delta I}{\delta t} . \qquad (46)$$

This is known as Fick's second law. It is this equation for which we must find a solution.

Our experimental arrangement is that of a radioactive layer of thickness h deposited on one end of a semi-infinite parallelo-

piped extending into the positive x direction. No diffusion can occur across the face x = 0. Further, at t = 0 all the radioactive atoms are concentrated uniformly in the radioactive layer, and none are present in the rest of the crystal. Accordingly, we can write our initial and boundary conditions as

$$I(x,0) = \begin{cases} I_0 & \text{for } x \leq h \quad (47) \\ 0 & \text{for } x > h \quad (48) \end{cases}$$

$$\frac{\delta I}{\delta x}(0,t) = 0$$

Equation (46) can be solved by means of the standard method of separation of variables. The solution can be written in the form

$$I(x,t) = \left[c_1(\alpha)\cos\alpha x + c_2(\alpha)\sin\alpha x\right] e^{-\alpha^2 Dt} \quad (49)$$

In view of condition (48) it can be seen at once that $c_2(\alpha)=0$. The most general solution will be a superposition of solutions of the form (49) over all positive values of α. It can be written as

$$I(x,t) = \int_0^\infty c_1(\alpha)\cos\alpha x \; e^{-\alpha^2 Dt} \, d\alpha \quad (50)$$

We next calculate $c_1(\alpha)$. Starting with

$$I(x,0) = \int_0^\infty c_1(\alpha)\cos\alpha x \, d\alpha \quad (51)$$

we obtain, using the Fourier Integral Theorem,

$$c_1(\alpha) = \frac{2}{\pi}\int_0^\infty c(x',0)\cos\alpha x' dx' = \frac{2}{\pi}\int_0^h I_0\cos\alpha x' dx' \quad (52)$$

the last identity following from (47). Thus we can rewrite (50) as

$$I(x,t) = \frac{2}{\pi}\int_0^h \left[\int_0^\infty I_0\cos\alpha x'\cos\alpha x \; e^{-\alpha^2 Dt} d\alpha\right] dx' \quad (53)$$

The integral in the brackets can be evaluated using the trigometric identity

$$2\cos\alpha x'\cos\alpha x = \cos\alpha(x'-x) + \cos\alpha(x'+x) \tag{54}$$

and Formula 508 in Peirce's Integral Tables. As a result, (53) becomes

$$I(x,t) = \frac{I_o}{2\sqrt{\pi Dt}} \int_{x-h}^{x+h} e^{\frac{-(x')^2}{4Dt}}\, dx' \tag{56}$$

While (56) is the exact solution to the diffusion equation (46), it is not readily suitable for evaluation of D from the experimental data. It will be recalled that such data are in the form of log radioactivity vs. $(\text{depth})^2$ curves. If the thickness h of the original radioactive layer is small compared to the total depth of diffusion, we can make the approximation

$$\int_{x-h}^{x+h} e^{\frac{(x')^2}{4Dt}}\, dx' \approx 2he^{-\frac{x^2}{4Dt}} \tag{57}$$

The error introduced through this approximation will be discussed below. In view of (56) and (57) we can write

$$\ln I = \ln \frac{hI_o}{\sqrt{\pi Dt}} - \frac{x^2}{4Dt} = \ln \frac{hI_o}{\sqrt{\pi Dt}} - \frac{(n\lambda)^2}{4Dt} \tag{58}$$

where λ is the thickness of one slice and n the depth in the crystal in units of λ. By choosing two slices a and b in the crystal, at depths n_a and n_b and with activities I_a and I_b, we can derive an expression for D from (58). It is given by

$$D = \frac{1}{4t} \frac{n_b^2 - n_a^2}{\ln I_a - \ln I_b} \lambda^2 \tag{59}$$

which is identical with (19). This expression is suitable for the calculation of D from the experimental data.

We must now consider more closely the approximations made by using eq (57). Generally speaking, this equation means approximating an area under a Gaussian curve by a rectangle, both being centered about the same ordinate and both having width h. It can be seen at once that the smaller the value of h, the better the approximation will be. For h = 0 the exact solution equals the approximate solution. However, the product Dt also is of importance. If we regard the Gaussian curve as invariant the interval of integration will contract as Dt increases and vice versa. Thus the larger Dt the better the approximation will be.

Another source of error in D is the finite thickness of the slices. For the purpose of a log activity vs. $(\text{depth})^2$ plot it would be reasonable to consider the radioactivity I of a slice to be concentrated at or near the center of such a slice. However, in our plot of log I vs. n^2, n represents the depth measured always at the end of a slice. This error can be minimized by plotting log I vs. $(n-1/2)^2$ instead of log I vs. n^2.

The approximations and errors just discussed are shown graphically in Figures 15 and 16. Each Figure represents a different value of Dt. Curves 1 and 2 represent the logarithm of the exact solution for two different values of h, plotted against n^2. To obtain numerical values for these solutions, they were written in the form

$$\frac{I_0}{2\sqrt{\pi Dt}} \int_{x-h}^{x+h} e^{\frac{-(x')^2}{4Dt}}\, dx' = \frac{I_0}{2}\left[\operatorname{erf}\frac{h+x}{\sqrt{4Dt}} + \operatorname{erf}\frac{h-x}{\sqrt{4Dt}}\right] \qquad (60)$$

They could then be evaluated with the help of error function tables. Curves 3 and 4 show the logarithm of the approximate solution (as given by the right hand side of (57)) plotted against n^2 and $(n-1/2)^2$ respectively.

The units used for I in Figures 15 and 16 are arbitrary. All constants common to both exact and approximate solutions have been neglected. Since we are only interested in the slopes of the curves and not the absolute magnitude of log I, some of the curves have also been shifted up or down arbitrarily so as to allow the easiest comparison. The pertinent expressions and numerical values used in Figures 15 and 16 are listed in Table III.

Table III

Figure 15

	Dt	h	λ	x	n
Curve 1	6×10^{-6}cm^2	10^{-3}cm	5×10^{-4}cm	$n\lambda$	integer
Curve 2	6×10^{-6}cm^2	5×10^{-4}cm	5×10^{-4}cm	$n\lambda$	integer
Curve 3	6×10^{-6}cm^2	0	5×10^{-4}cm	$n\lambda$	integer
Curve 4	6×10^{-6}cm^2	0	5×10^{-4}cm	$(n - 1/2)\lambda$	integer

Figure 16

	Dt	h	λ	x	n
Curve 1	2×10^{-6}cm^2	10^{-3}cm	5×10^{-4}cm	$n\lambda$	integer
Curve 2	2×10^{-6}cm^2	5×10^{-4}cm	5×10^{-4}cm	$n\lambda$	integer
Curve 3	2×10^{-6}cm^2	0	5×10^{-4}cm	$n\lambda$	integer
Curve 4	2×10^{-6}cm^2	0	5×10^{-4}cm	$(n - 1/2)\lambda$	integer

Inspection of curve 1 in Figures 15 and 16 reveals a considerable deviation from a straight line at low values of n^2. This deviation is due to the relatively large value of h. In curve 2,

where h is half this value, the deviation has largely disappeared. Comparing either 1 or 2 with either 3 or 4 we notice that the slopes of the exact solution are always steeper than those of the approximate solution. Similarly, 4 always has a steeper slope than 3. However, all the curves have a tendency to straighten out and become more parallel as n^2 increases. This is to be expected, since the error due to h is a surface effect and since the relative difference between $(n-1/2)^2$ and n^2 will decrease with increasing n^2.

The numerical values shown in Table III correspond to typical experimental situations. To give an idea of how the various approximation affect our experimental results, Table IV lists the percentage errors in D which occur due to these approximations. In each case D has been computed from the slopes of two of the curves in Figures 15 and 16 and the percentage difference calculated.

Table IV

Approximation	% error in D ($Dt = 6\times10^{-6}$ cm^2)	($Dt = 2\times10^{-6}$ cm^2)
3 instead of 1	4%	6%
3 instead of 2	1%	2%
4 instead of 1	2%	3%
4 instead of 2	1%	2%

It should be pointed out that the slopes for the case $Dt = 2\times10^{-6}$ cm^2 were measured at somewhat lower values of n^2 than for the case $Dt = 6\times10^{-6}$ cm^2. This is in line with experimental conditions, since the former case generally will not yield as many measurable slices as the latter. Had the slopes been compared at the same values of n^2, there would have been very little difference

between the two cases. It is quite apparent from Table IV, however, that the largest error comes from using too thick a radioactive layer. By minimizing the thickness of this layer and also the thickness of a slice and by taking as many slices as possible, the errors in D due to the above approximations can be made quite small compared to the experimental errors.

Figure 1. Two-dimensional representation of various lattice defects

A. Perfect lattice

B. Frenkel defects (vacancies and interstitial ions)

C. Schottky defects (positive and negative ion vacancies)

D. Divalent ion in lattice (divalent positive ion replacing monovalent positive ion and creating positive ion vacancy)

E. Complex in lattice (divalent positive ion and positive ion vacancy bound together)

F. Paired vacancies (positive and negative ion vacancies bound together)

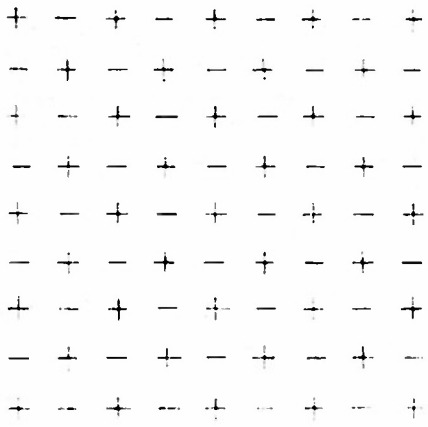

A. PERFECT LATTICE

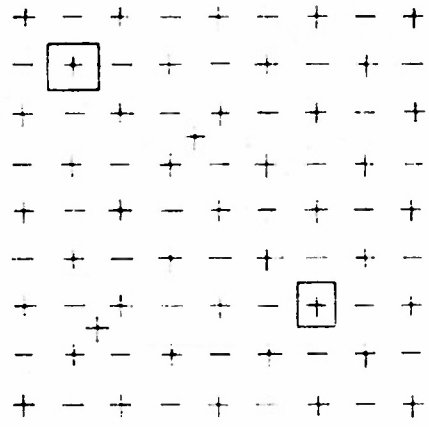

B. FRENKEL DEFECTS

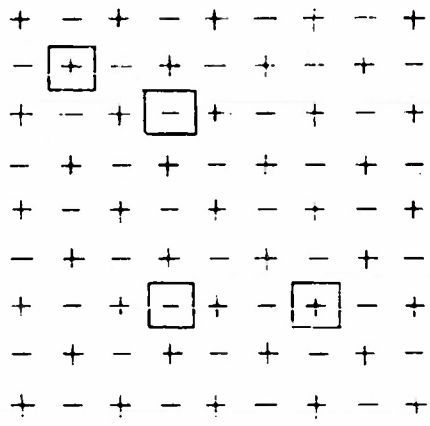

C. SCHOTTKY DEFECTS

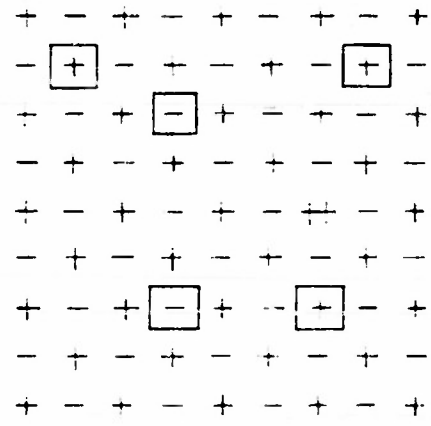

D. DIVALENT ION IN LATTICE

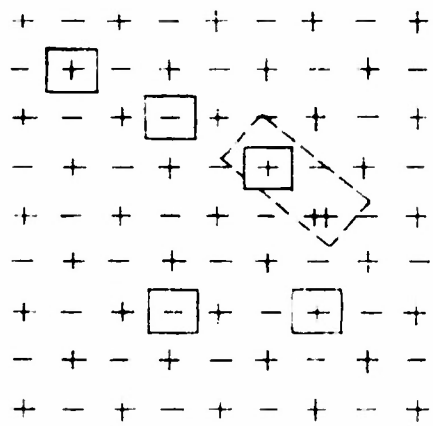

E. COMPLEX IN LATTICE

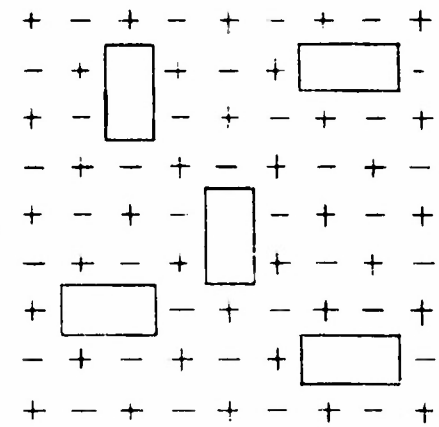

F. PAIRED VACANCIES

Figure 2. Experimental arrangement for diffusion

A. Alkali halide specimens

B. Platinum capsule covering specimens

C. Evaporated layer of radioactive material (exaggerated)

D. Platinum spacer to separate specimens (exaggerated)

E. Vycer capusle (filled with helium)

F. Thin coating of same material as specimen

G. Capsule holder (thin-walled stainless steel tube, closed off at bottom and connected to brass disk at top)

H. Chromel-Alumel thermocouple

For an actual diffusion experiment the holder is inserted into a vacuum tight quartz tube running through a Hoskins furnace.

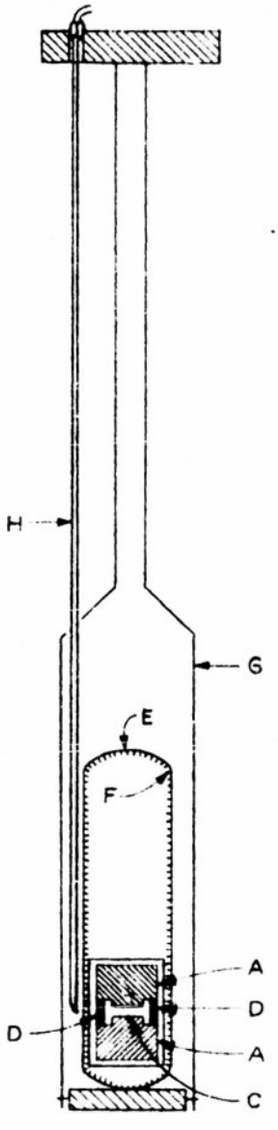
H
G
E
F
A
D
D
A
C

Figure 3. Holder for conductivity measurements

A. Solid platinum electrodes

B. Vycor tube (6 mm OD)

C. Vycor tube (22 mm OD)

D. Steel springs (the attached platinum wires constitute the ground lead)

E. Platinum-Platinum Rhodium (10 %) thermocouple

F. Platinum wire (high lead)

G. Stupakoff seal

H. Amphenol socket

I. Sample (actual size: 1 mm x 2 mm x 2 mm, the 1 mm dimension being the one separating the two electrodes)

For actual conductivity measurements the holder is inserted into a vacuum tight quartz tube running through a Hoskins furnace and pure helium circulated through the tube and holder.

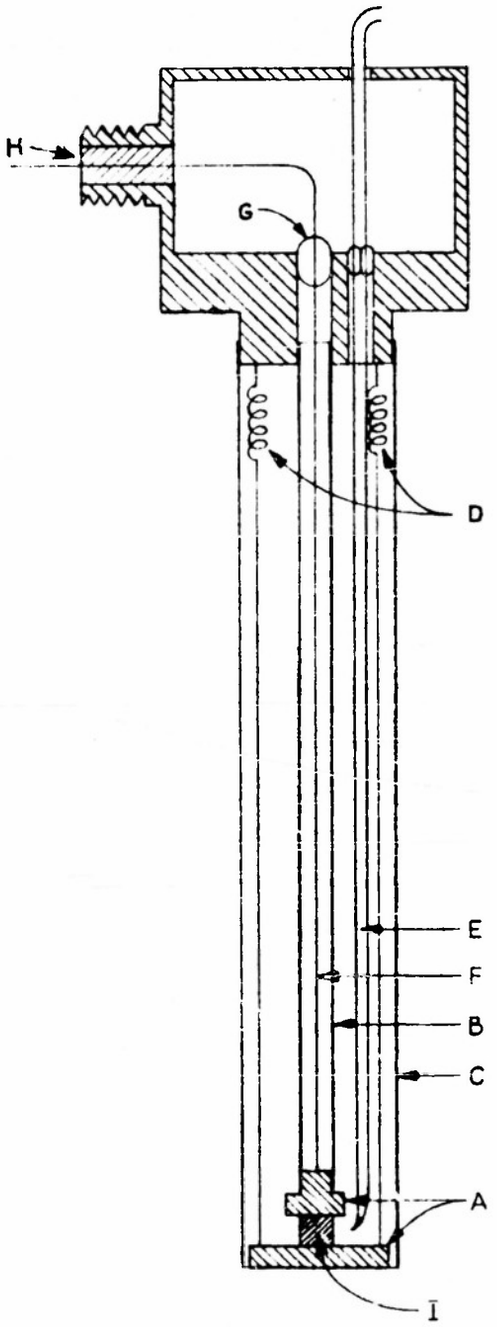
H
G
D
E
F
B
C
A
I

Figure 4. Schematic diagram of the bridge circuit

A. Hewlett-Packard audio-oscillator

B. General Radio 716-C bridge

C. Sample and sample holder

D. General Radio 736-A wave analyser

E. General Radio 722-D precision condenser

All the condensers and resistors shown inside the dotted square are contained within the bridge. All the other equipment is connected to the bridge externally.

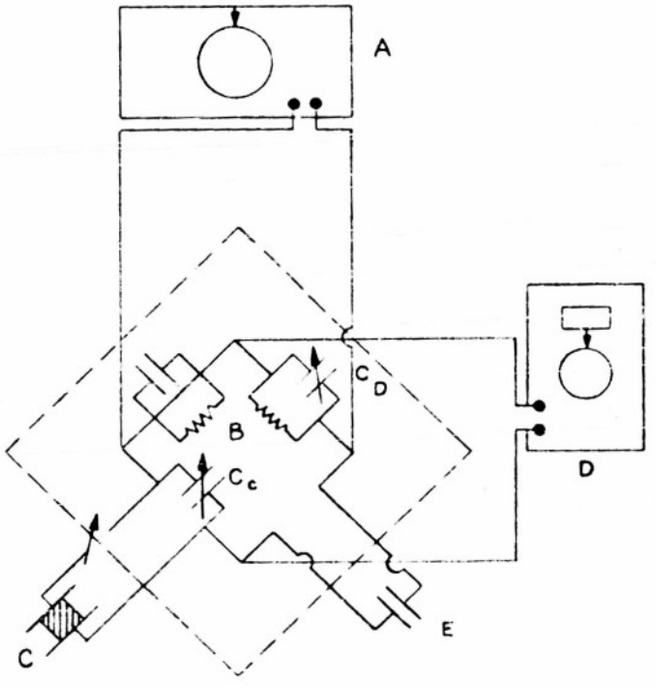
A
B
C_D
C_c
C
D
E

Figure 5. Typical plot of the logarithm of the radioactivity I of a slice (in counts per minute) versus the square of the slice number n. The upward deviation of the first few points is due to the finite thickness of the original radioactive layer.

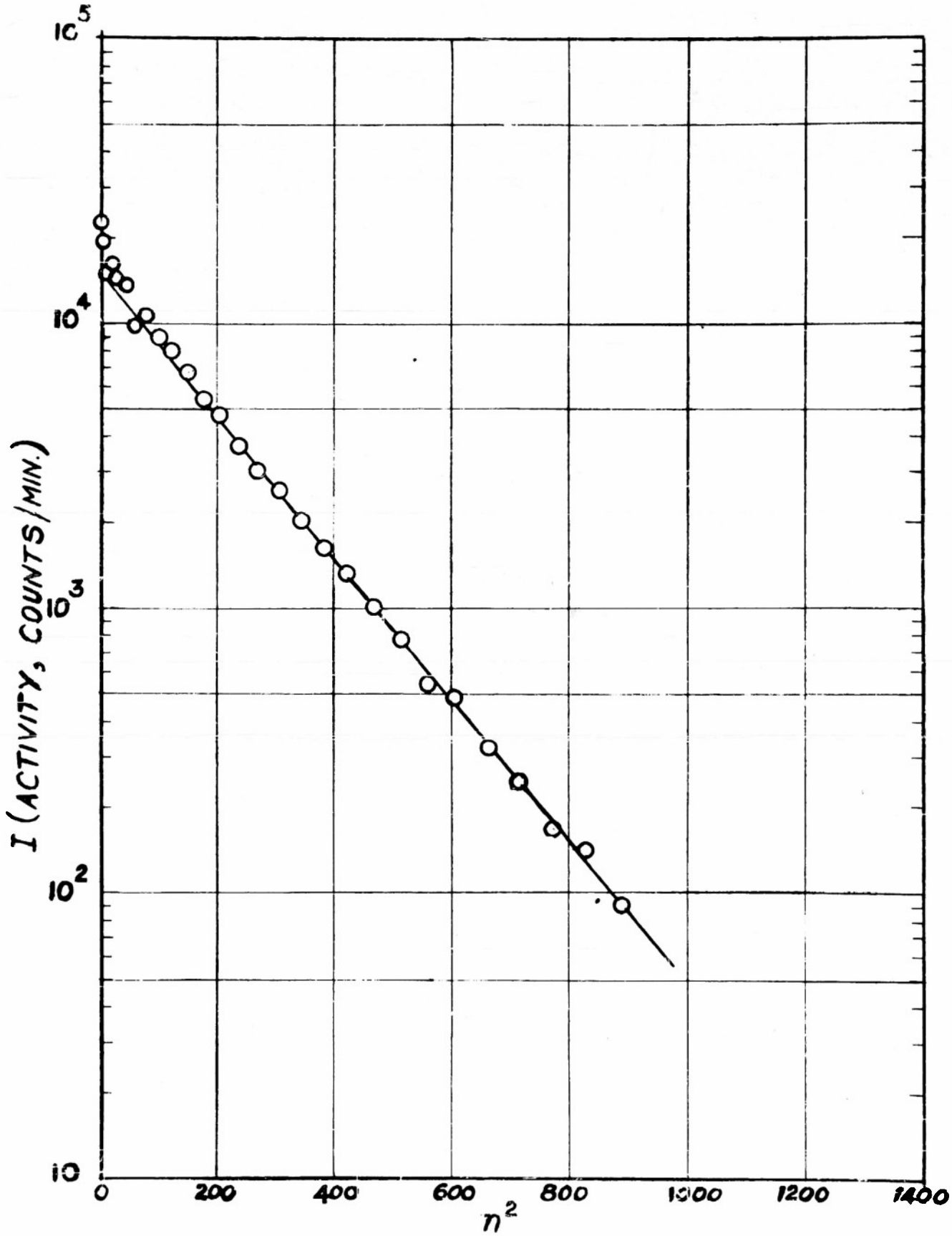
10^5
10^4
10^3
10^2
10
I (ACTIVITY, COUNTS/MIN.)
0
200
400
600
800
1000
1200
1400
n^2

Figure 6. Degree of association p calculated as a function of T/T_o for single crystals of NaCl + $CdCl_2$ (molar ratio $\frac{Cd}{Na} = 30 \times 10^{-5}$)

T = absolute temperature

T_o = energy of association (in units of Boltzmann's constant) = 3900°K

Solid curve: p calculated on the basis of equation (11)

Dashed curve: p calculated on the basis of equation (7)

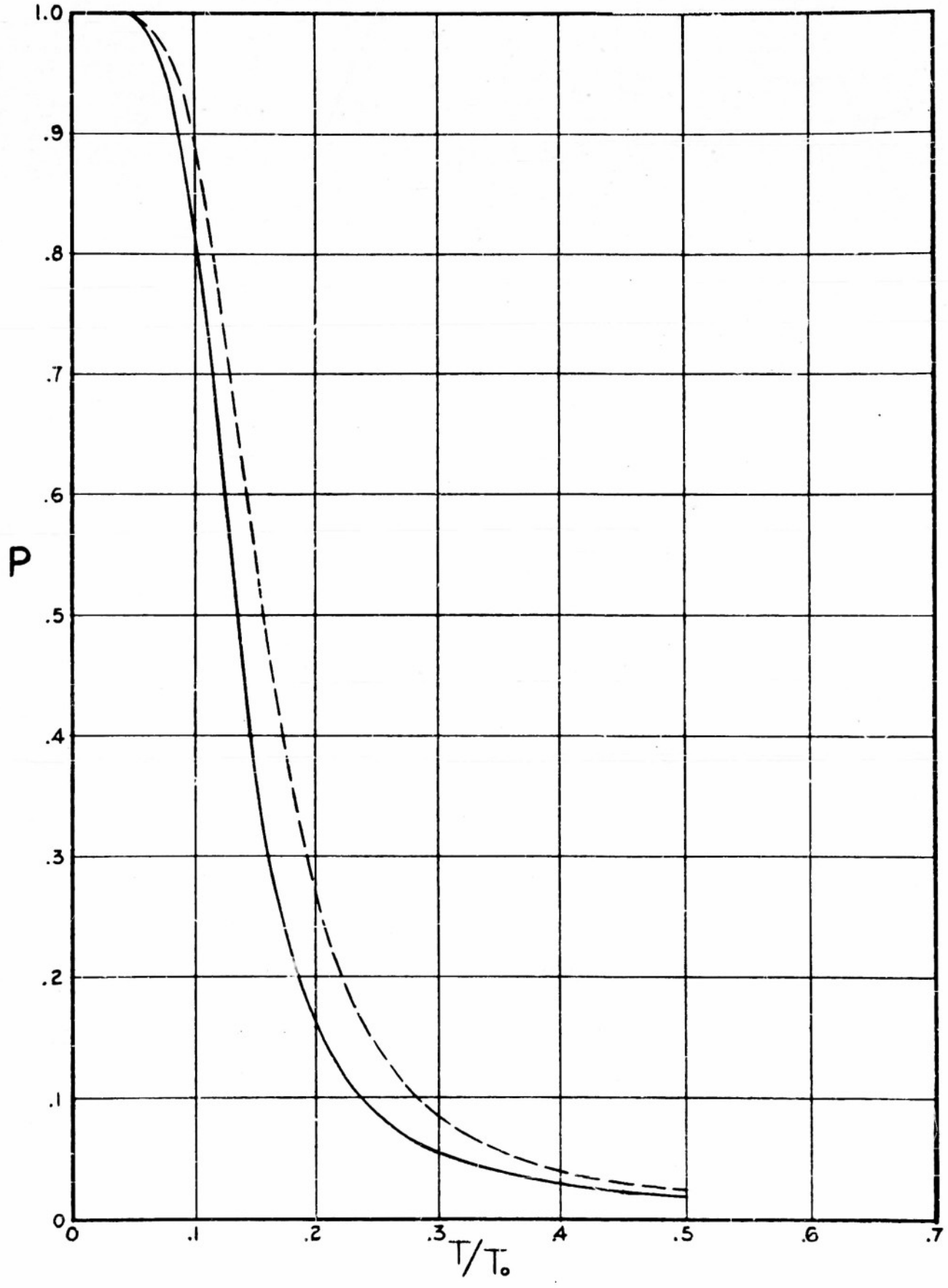
1.0
.9
.8
.7
.6
P
.5
.4
.3
.2
.1
0
0
.1
.2
.3
.4
.5
.6
.7
T/T₀

Figure 7. Degree of association p calculated as a function of T/T_o for single crystals of NaCl + $CdCl_2$ (molar ratio $\frac{Cd}{Na} = 14 \times 10^{-5}$)

T = absolute temperature

T_o = energy of association (in units of Boltzmann's constant) = 3900°K

Solid curve: p calculated on the basis of equation (11)

Dashed curve: p calculated on the basis of equation (7)

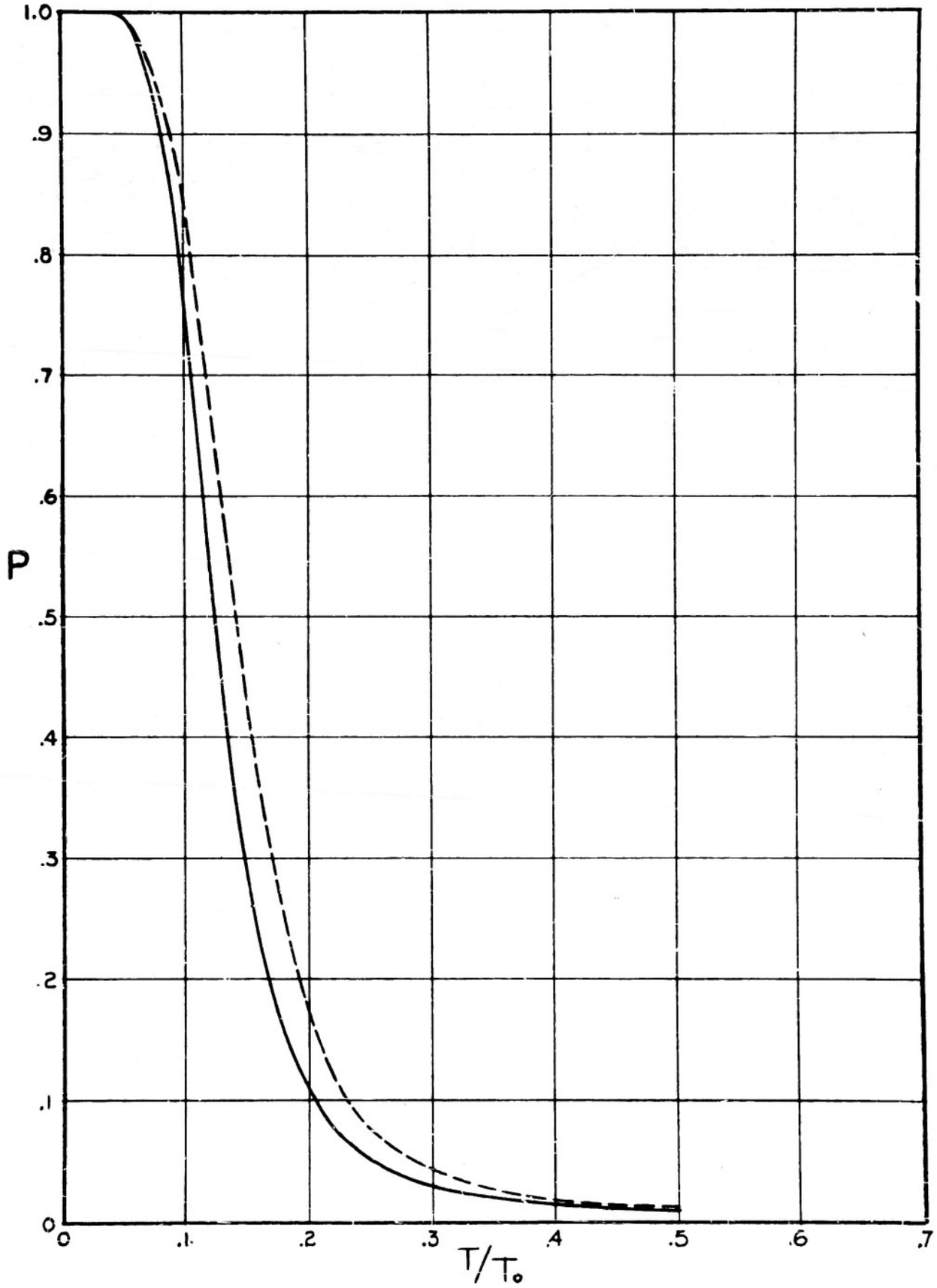
1.0
.9
.8
.7
.6
P
.5
.4
.3
.2
.1
0
0
.1
.2
.3
.4
.5
.6
.7
T/T₀

Figure 8. Degree of association p calculated as a function of T/T_o for single crystals of NaCl + $CdCl_2$ (molar ratio $\frac{Cd}{Na} = 4 \times 10^{-5}$)

T = absolute temperature

T_o = energy of association (in units of Boltzmann's constant) = 3900°K

Solid curve: p calculated on the basis of equation (11)

Dashed curve: p calculated on the basis of equation (7)

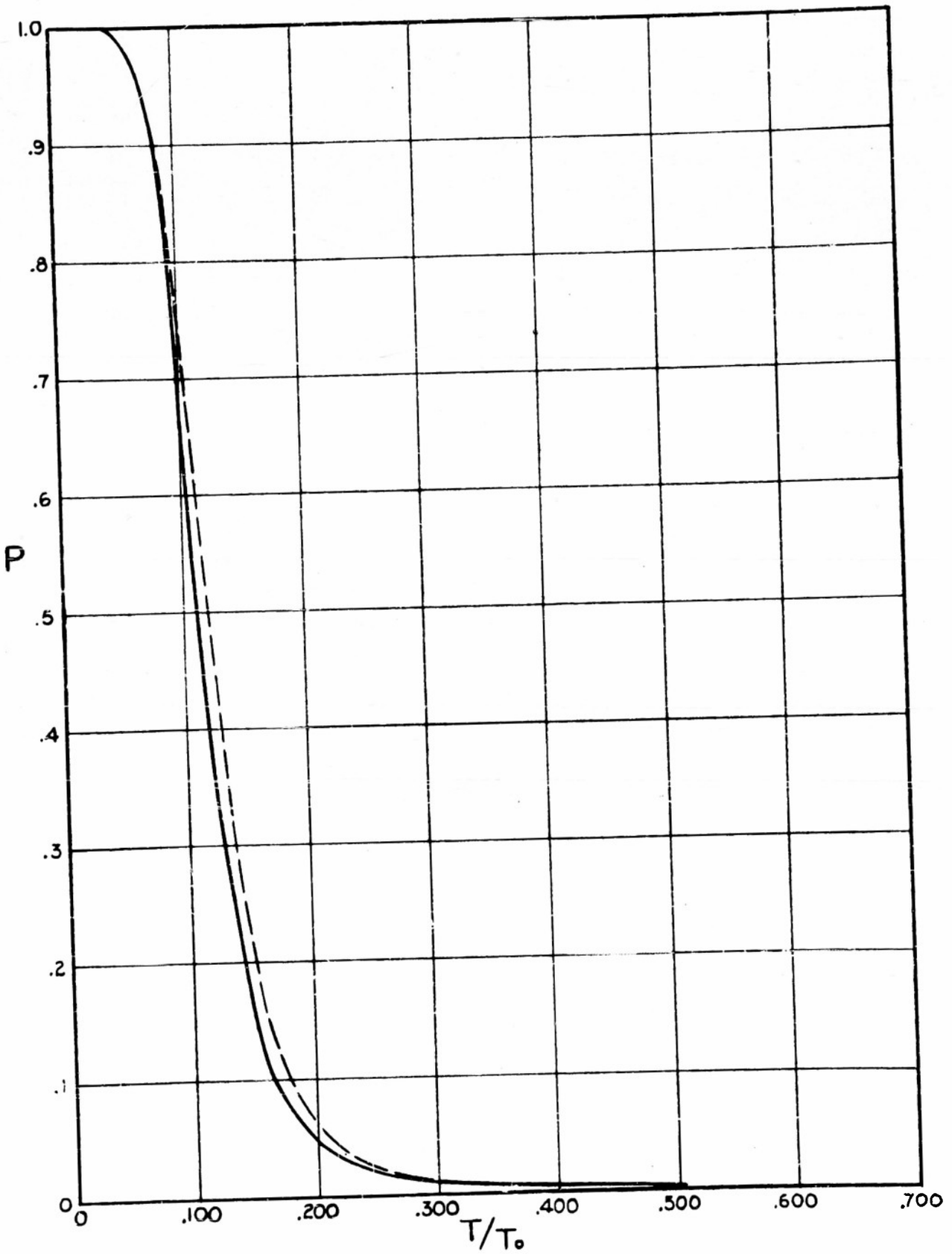
1.0
.9
.8
.7
.6
P
.5
.4
.3
.2
.1
0
0
.100
.200
.300
.400
.500
.600
.700
T/T₀

Figure 9. Degree of association p calculated as a function of T/T_o for single crystals of NaCl + $CdCl_2$ (molar ratio $\frac{Cd}{Na} = .5 \times 10^{-5}$)

T = absolute temperature

T_o = energy of association (in units of Boltzmann's constant) = 3900°K

Solid curve: p calculated on the basis of equation (11)

Dashed curve: p calculated on the basis of equation (7)

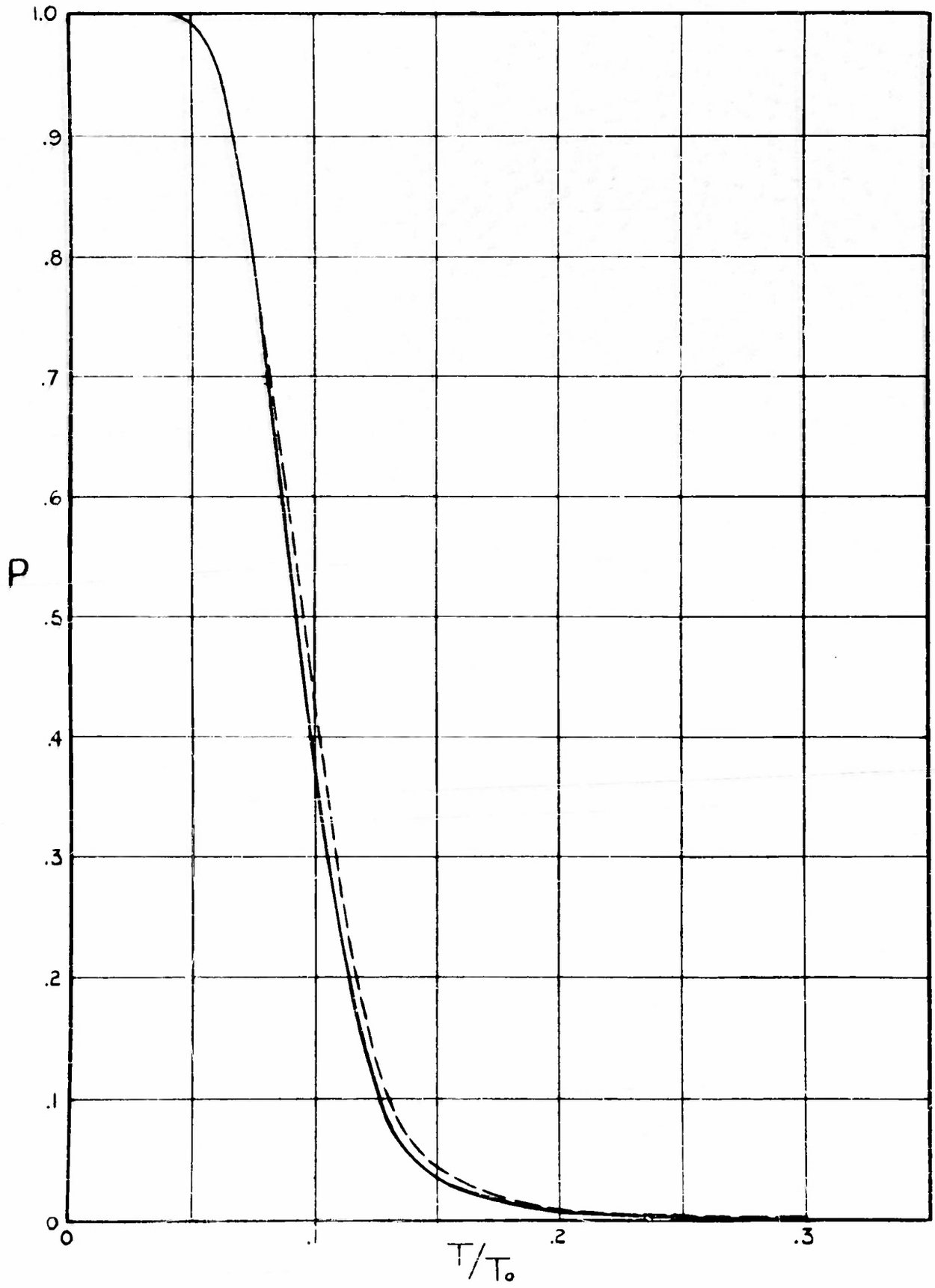
1.0
.9
.8
.7
.6
P
.5
.4
.3
.2
.1
0
0
.2
.3
T/T₀

Figure 10. Conductivity σ ($ohm^{-1}cm^{-1}$) in single crystals of $NaCl + CdCl_2$ as a function of the inverse absolute temperature, for various molar ratios $\frac{Cd}{Na}$.

A. Molar ratio $\frac{Cd}{Na} = 30 \times 10^{-5}$

B. Molar ratio $\frac{Cd}{Na} = 14 \times 10^{-5}$

C. Molar ratio $\frac{Cd}{Na} = 4 \times 10^{-5}$

D. Molar ratio $\frac{Cd}{Na} = .5 \times 10^{-5}$

E. Molar ratio $\frac{Cd}{Na} =$ -- ("pure" NaCl)

Each specimen was put through the same temperature cycle. The upper curve for each crystal refers to conductivities measured during the first half of the cycle (temperature increasing) and the lower curve to conductivities measured during the second half of the cycle (temperature decreasing). For "pure" NaCl (E) the two curves coincide.

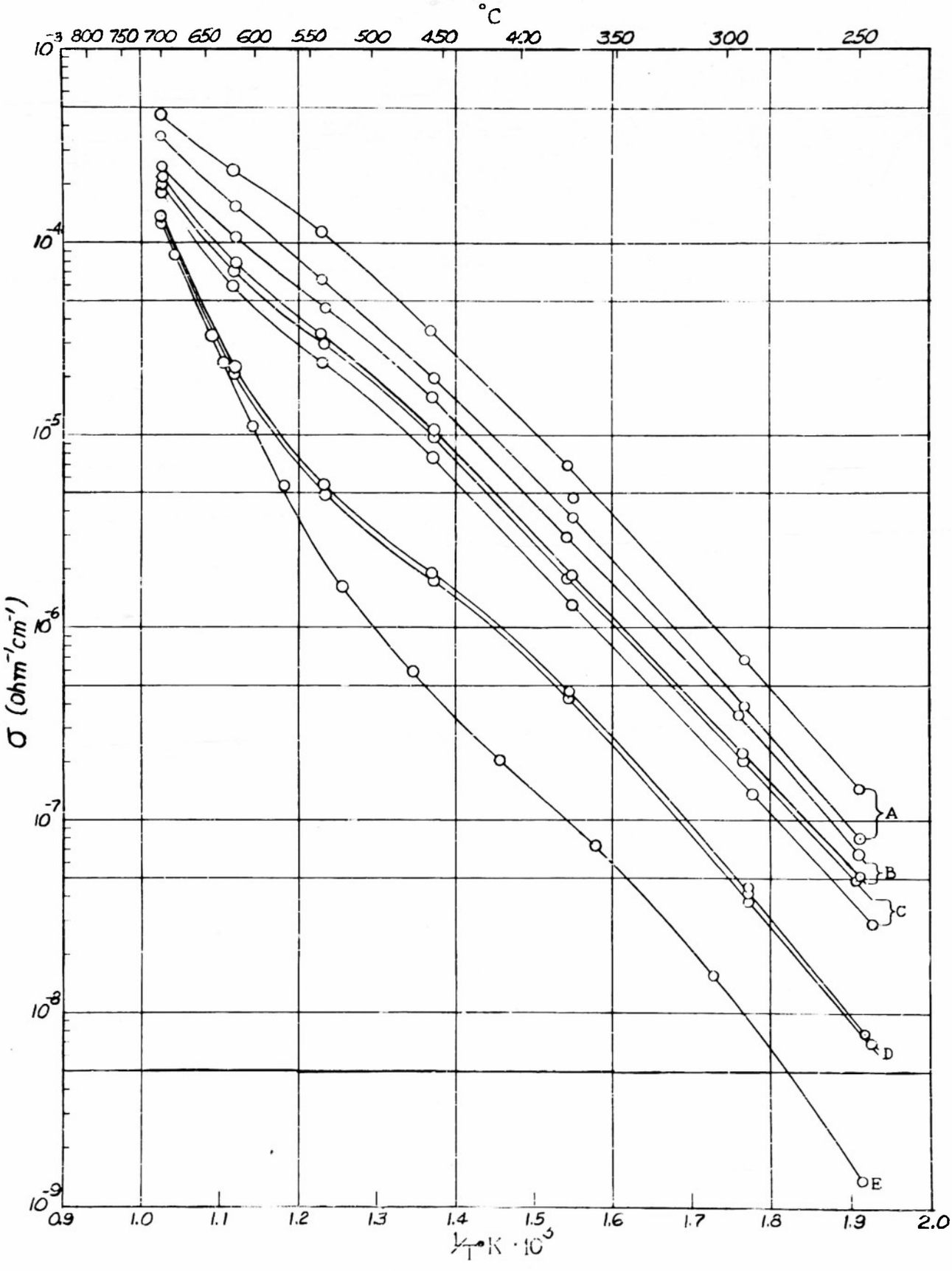
°C
800 750 700 650 600 550 500 450 400 350 300 250
10^{-3}
10^{-4}
10^{-5}
10^{-6}
10^{-7}
10^{-8}
10^{-9}
σ (ohm⁻¹cm⁻¹)
0.9 1.0 1.1 1.2 1.3 1.4 1.5 1.6 1.7 1.8 1.9 2.0
1/T °K · 10³
A
B
C
D
E

Figure 11. Calculated and measured self diffusion coefficients D (cm^2/sec) of Na^+ in single crystals of NaCl + $CdCl_2$ (molar ratio $Cd/Na = 30 \times 10^{-5}$) as a function of the inverse absolute temperature. To calculate diffusion coefficients from conductivities the Einstein relation was used.

Solid curve: self diffusion coefficient calculated from the measured conductivity

Dotted curve: self diffusion codfficient calculated from the conductivity resulting if there were no association (p calculated using equation (7))

Dashed curve: self diffusion coefficient calculated from the conductivity resulting if there were no association (p calculated using equation (11))

Circles: self diffusion coefficient measured by radioactive tracer

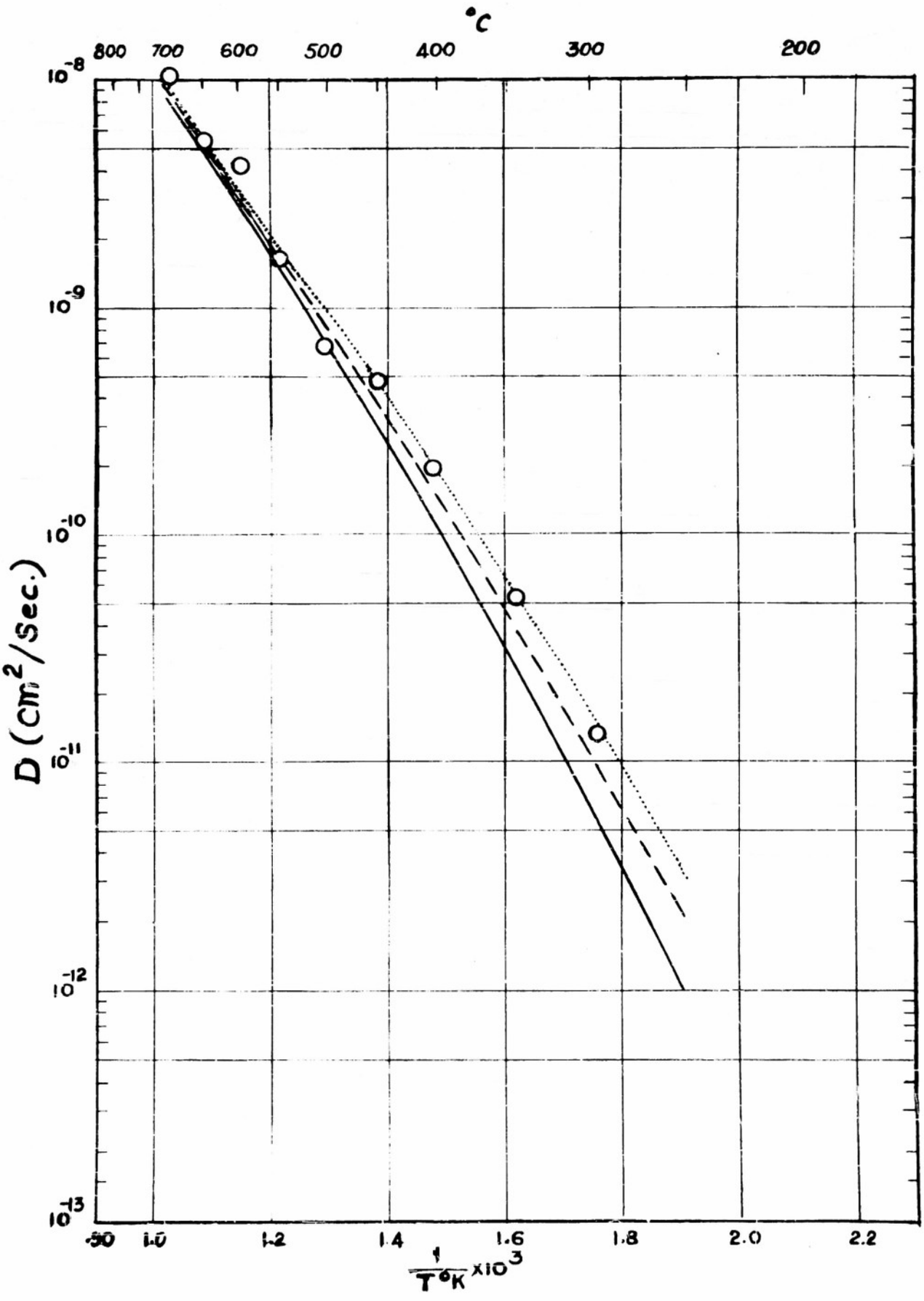
°C
800
700
600
500
400
300
200
10^{-8}
10^{-9}
10^{-10}
10^{-11}
10^{-12}
10^{-13}
D (Cm²/Sec.)
.90
1.0
1.2
1.4
1.6
1.8
2.0
2.2
$\frac{1}{T°K} \times 10^{3}$

Figure 12. Calculated and measured self diffusion coefficients D (cm^2/sec) of Na^+ in single crystals of NaCl + $CdCl_2$ (molar ratio $Cd/Na = 14 \times 10^{-5}$) as a function of the inverse absolute temperature. To calculate diffusion coefficients from conductivities the Einstein relation was used.

Solid curve: self diffusion coefficient calculated from the measured conductivity

Dotted curve: self diffusion coefficient calculated from the conductivity resulting if there were no association (p calculated using equation (7))

Dashed curve: self diffusion coefficient calculated from the conductivity resulting if there were no association (p calculated using equation (11))

Circles: self diffusion coefficient measured by radioactive tracer

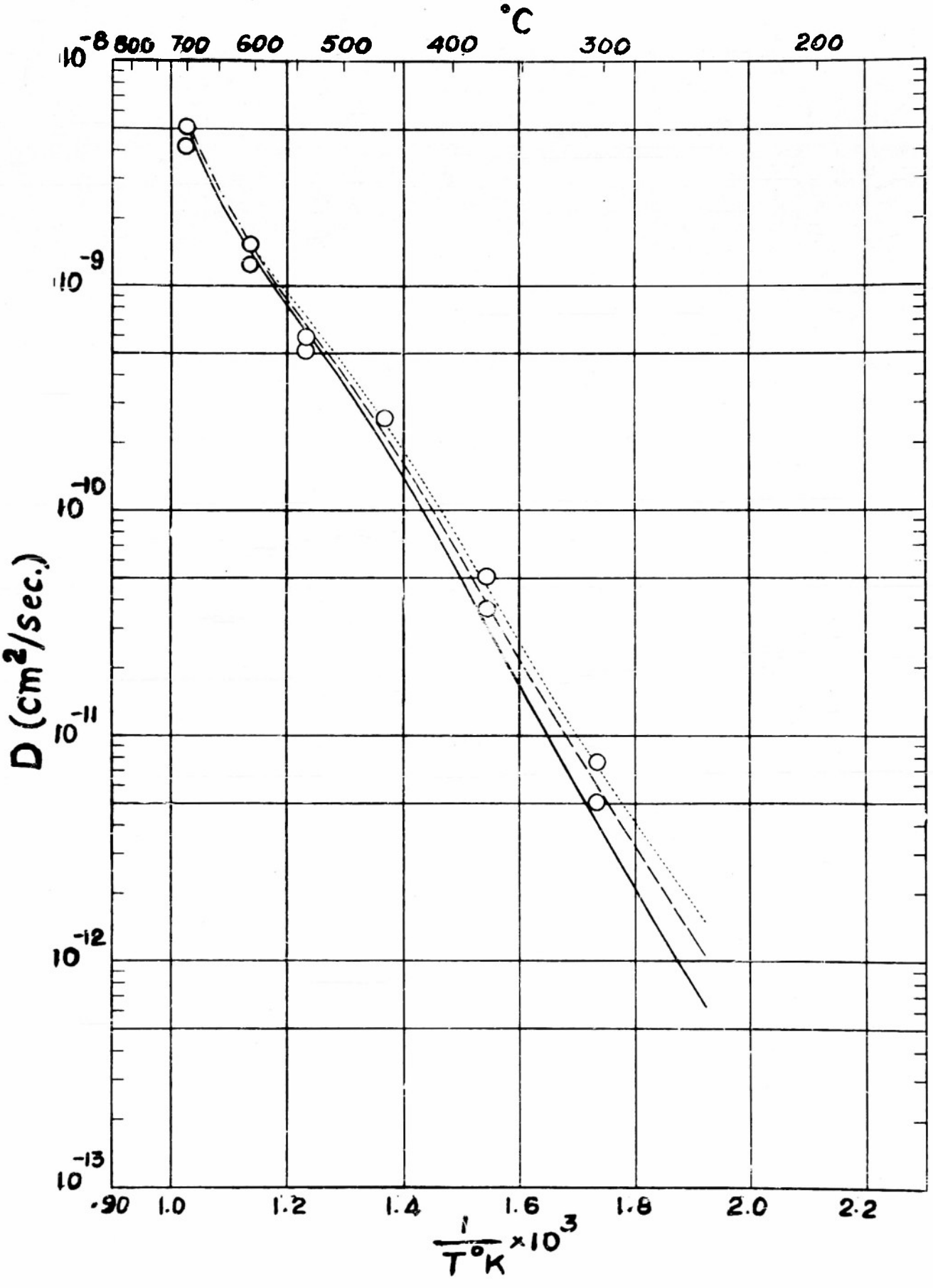
°C
800
700
600
500
400
300
200
10^{-8}
10^{-9}
10^{-10}
10^{-11}
10^{-12}
10^{-13}
D (cm²/Sec.)
.90
1.0
1.2
1.4
1.6
1.8
2.0
2.2
$\frac{1}{T°K} \times 10^3$

Figure 13. Calculated and measured self diffusion coefficients D (cm^2/sec) of Na^+ in single crystals of NaCl + $CdCl_2$ (molar ratio $Cd/Na = 4 \times 10^{-5}$) as a function of the inverse absolute temperature. To calculate diffusion coefficients from conductivities the Einstein relation was used.

Solid curve: self diffusion coefficient calculated from the measured conductivity

Dotted curve: self diffusion coefficient calculated from the conductivity resulting if there were no association (ρ calculated using equation (7))

Dashed curve: self diffusion coefficient calculated from the conductivity resulting if there were no association (ρ calculated using equation (11))

Circles: self diffusion coefficient measured by radicactive tracer

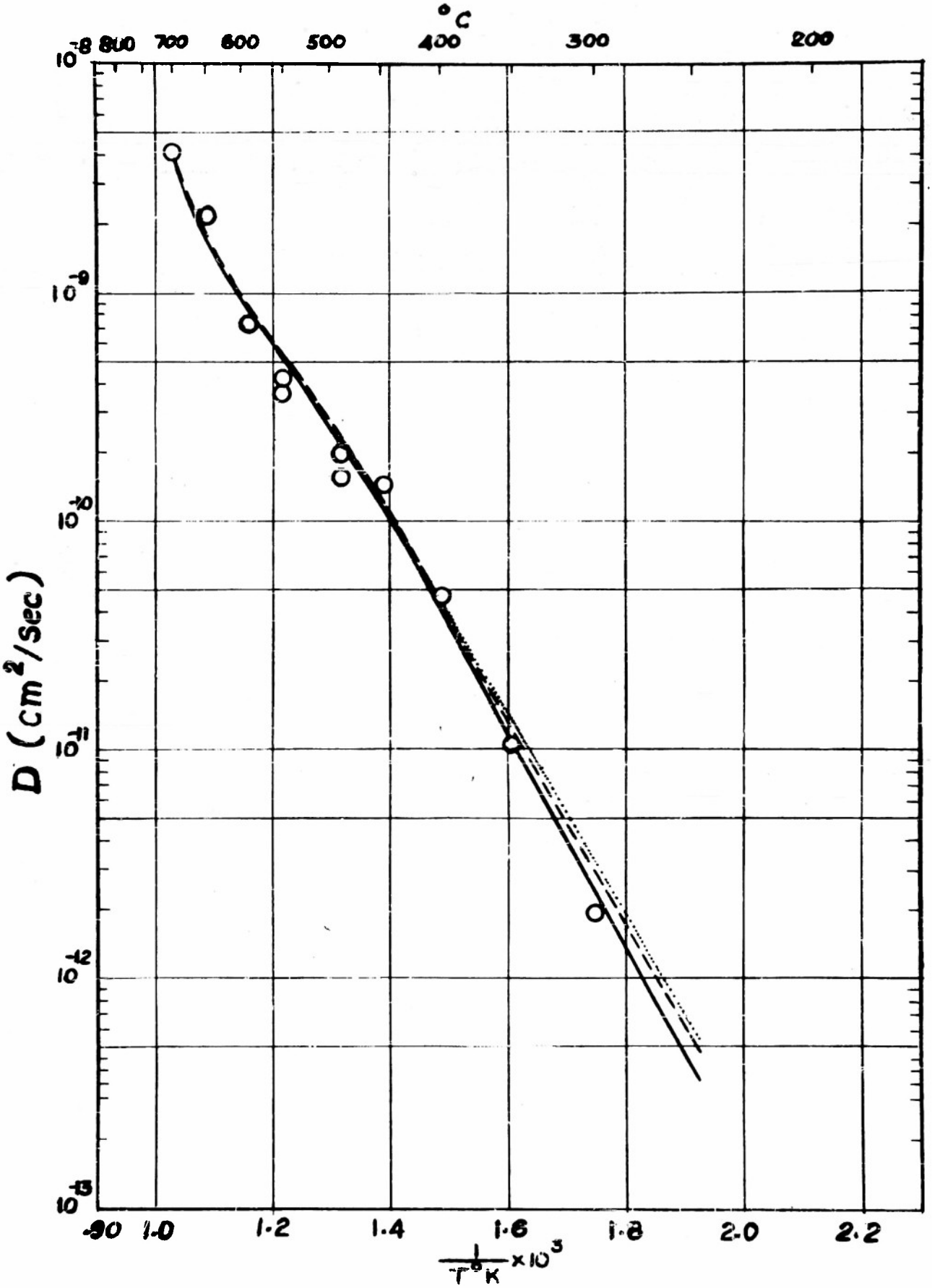
°C
800
700
600
500
400
300
200
10^{-8}
10^{-9}
10^{-10}
10^{-11}
10^{-12}
10^{-13}
D (cm²/Sec)
.90
1.0
1.2
1.4
1.6
1.8
2.0
2.2
$\frac{1}{T°K} \times 10^3$

Figure 14. Calculated and measured self diffusion coefficients D (cm^2/sec) of Na^+ in single crystals of NaCl + $CdCl_2$ (molar ratio $Cd/Na = .5 \times 10^{-5}$) as a function of the inverse absolute temperature. To calculate diffusion coefficients from conductivities the Einstein relation was used.

Solid curve: self diffusion coefficient calculated from the measured conductivity

D-- dashed curve: self diffusion coefficient calculated from the conductivity resulting if there were no association (p calculated using either equation (7) or (11).)

Circles: self diffusion coefficient measured by radioactive tracer.

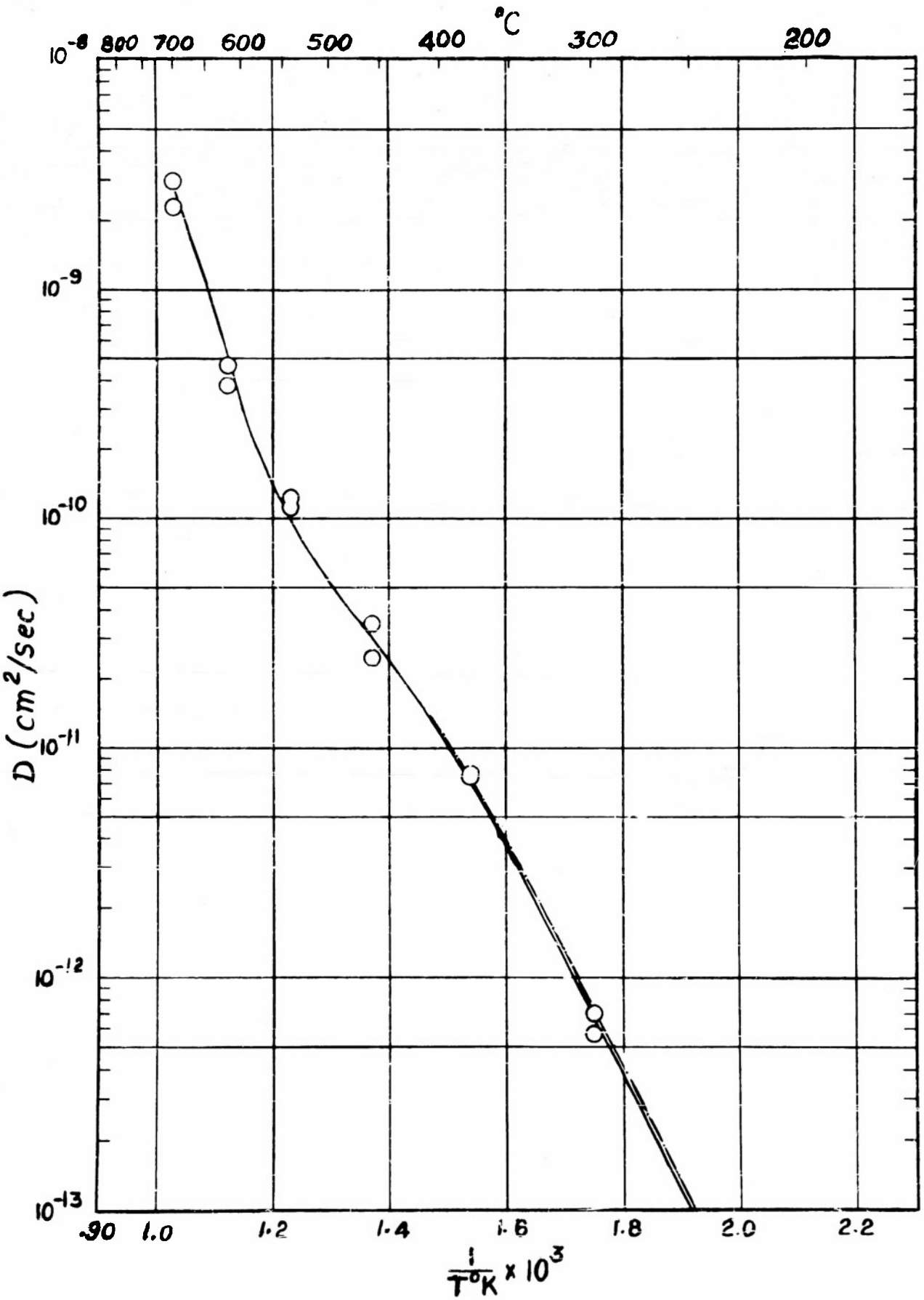
°C
800
700
600
500
400
300
200
10^{-8}
10^{-9}
10^{-10}
10^{-11}
10^{-12}
10^{-13}
D (cm²/Sec)
.90
1.0
1.2
1.4
1.6
1.8
2.0
2.2
$\frac{1}{T°K} \times 10^3$

Figure 15. Solutions of the diffusion equation

Curve 1: logarithm of exact solution ($h=10^{-3}$ cm) plotted against n^2

Curve 2: logarithm of exact solution ($h=5\times10^{-4}$ cm) plotted against n^2

Curve 3: logarithm of approximate solution ($h=0$) plotted against n^2

Curve 4: logarithm of approximate solution ($h=0$) plotted against $(n-1/2)^2$

h = thickness of original radioactive layer

n = slice number

The units used for the solution of the diffusion equation are arbitrary. Some of the curves have been shifted up or down to permit easier comparison of their slopes. All solutions were evaluated for $Dt = 6\times10^{-6}$ cm^2, where D is the diffusion coefficient in cm^2/sec and t the diffusion time in seconds.

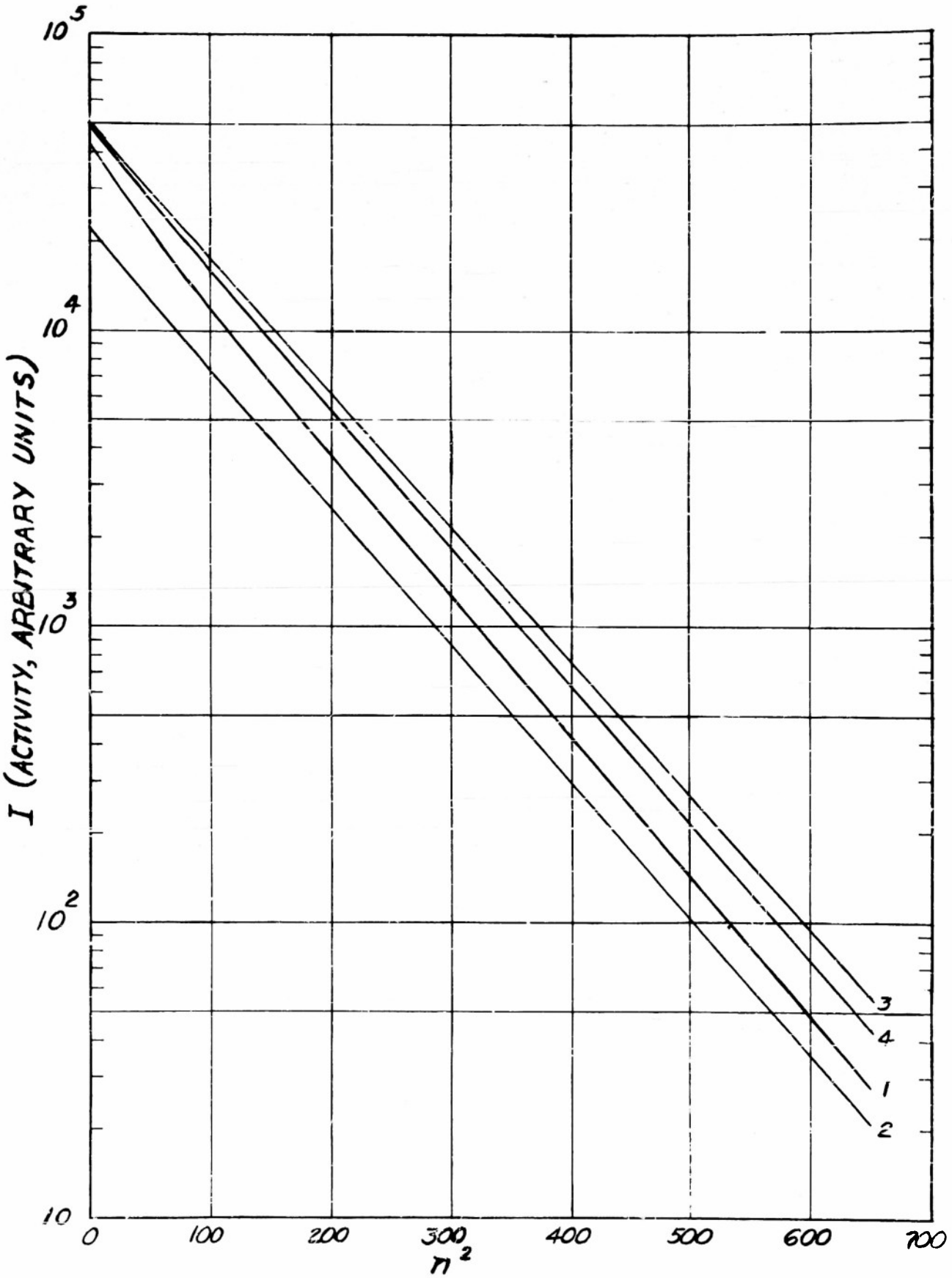
10^5
10^4
10^3
10^2
10
I (ACTIVITY, ARBITRARY UNITS)
0
100
200
300
400
500
600
700
n^2
3
4
1
2

Figure 16. Solutions of the diffusion equation

Curve 1: logarithm of exact solution ($h=10^{-3}$cm) plotted against n^2

Curve 2: logarithm of exact solution ($h=5\times10^{-4}$cm) plotted against n^2

Curve 3: logarithm of approximate solution ($h=0$) plotted against n^2

Curve 4: logarithm of approximate solution ($h=0$) plotted against $(n-1/2)^2$

h = thickness of original radioactive layer

n = slice number

The units used for the solution of the diffusion equation are arbitrary. Some of the curves have been shifted up or down to permit easier comparison of their slopes. All solutions were evaluated for $Dt = 2\times10^{-6}$ cm^2, where D is the diffusion coefficient in cm^2/sec and t the diffusion time in seconds.

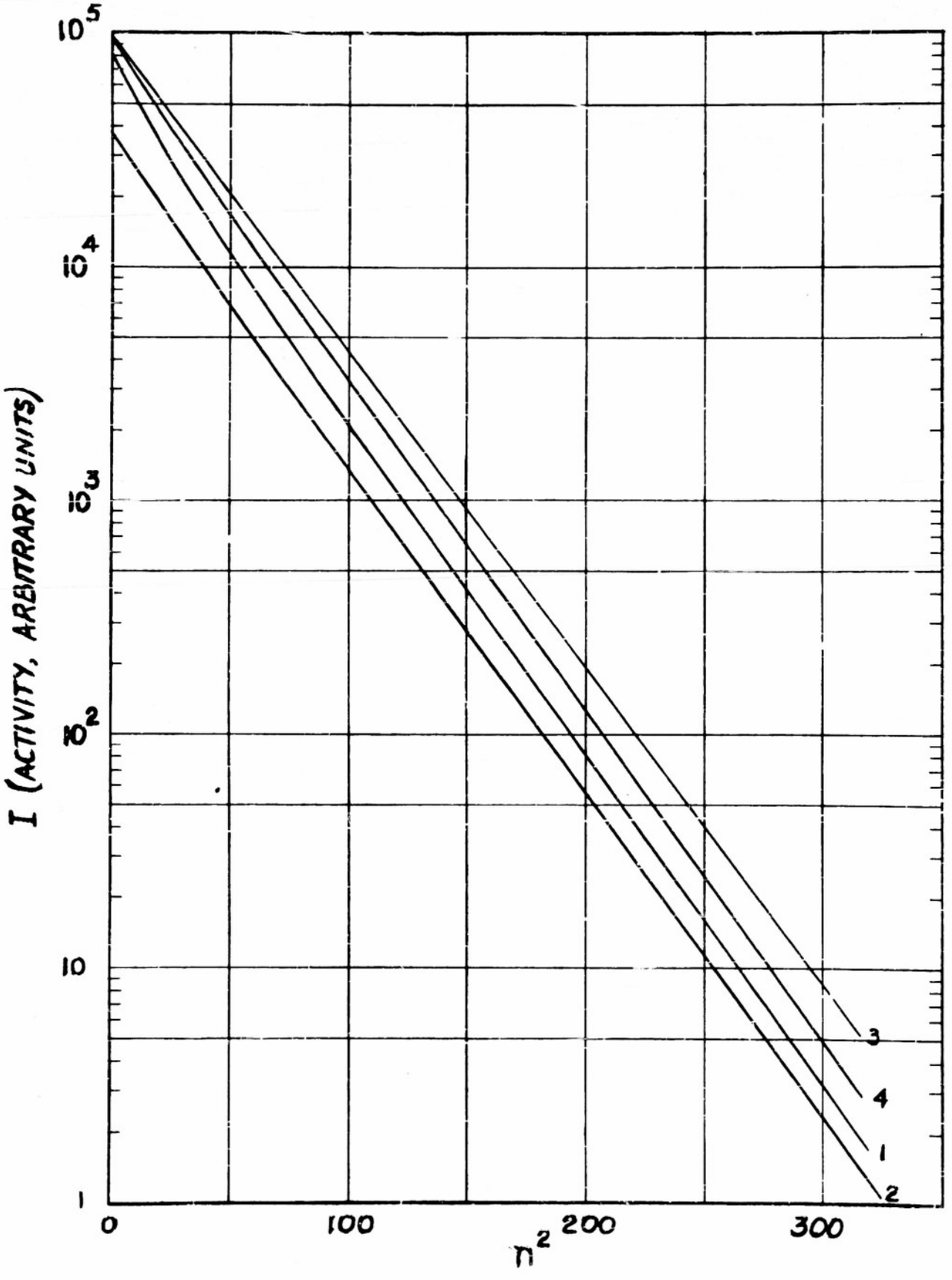
10^5
10^4
10^3
10^2
10
1
I (ACTIVITY, ARBITRARY UNITS)
0
100
200
300
n^2
3
4
1
2

Figure 17. Conductivity ($ohm^{-1}cm^{-1}$) in "pure" Harshaw KCl single crystals as a function of the inverse absolute temperature. The circles represent the results of actual measurements on four different specimens. The "knee" of the curve occurs at about 450°C.

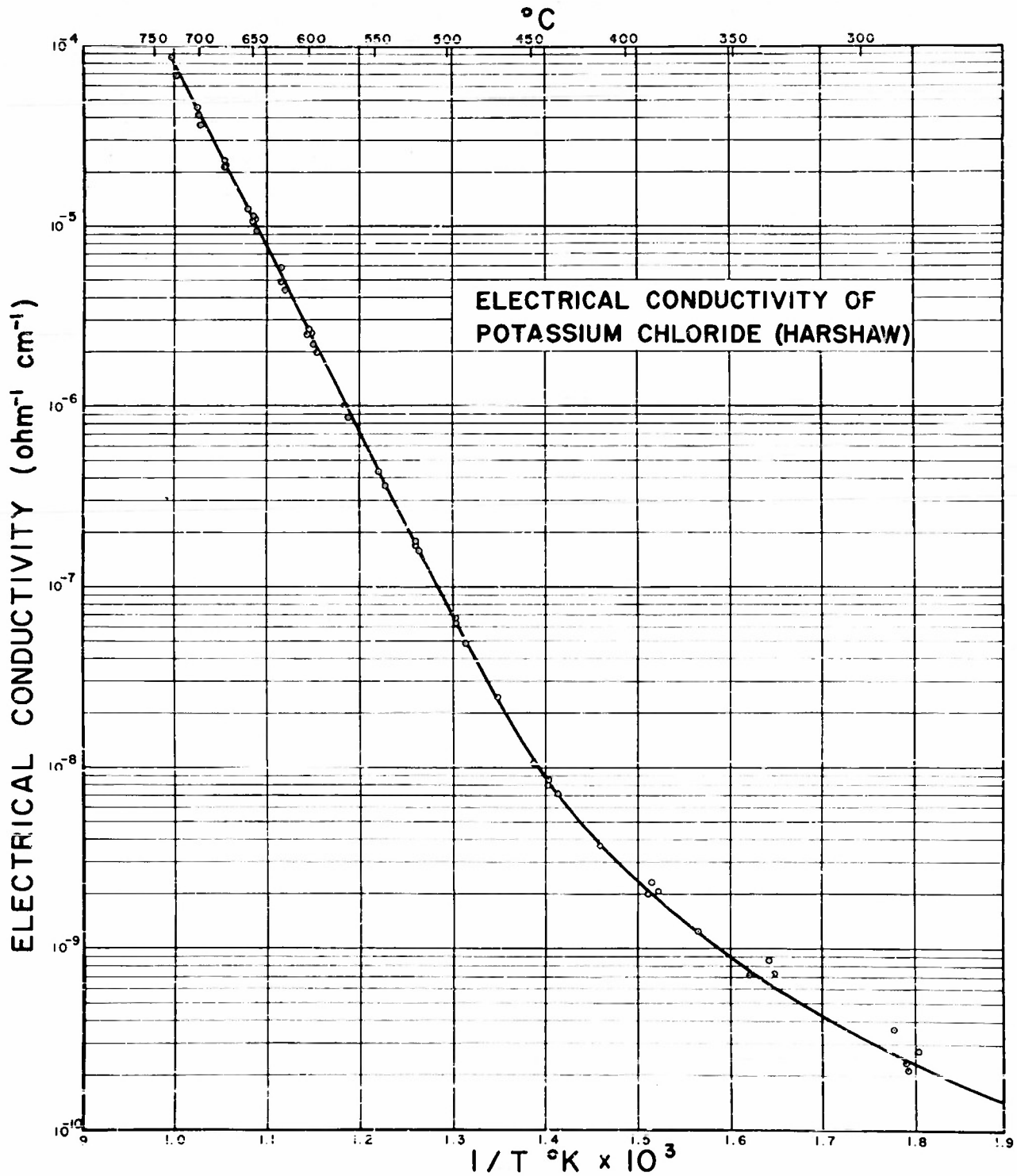
°C
750 700 650 600 550 500 450 400 350 300
ELECTRICAL CONDUCTIVITY OF
POTASSIUM CHLORIDE (HARSHAW)
ELECTRICAL CONDUCTIVITY (ohm⁻¹ cm⁻¹)
10⁻⁴
10⁻⁵
10⁻⁶
10⁻⁷
10⁻⁸
10⁻⁹
10⁻¹⁰
1.0 1.1 1.2 1.3 1.4 1.5 1.6 1.7 1.8 1.9
1/T °K x 10³

Figure 18. Calculated and measured self diffusion coefficients $D(cm^2/sec)$ of K^+ in "pure" Harshaw KCl single crystals as a function of the inverse absolute temperature. To calculate self diffusion coefficients from conductivities the Einstein relation was used.

Solid line: self diffusion coefficient calculated from the conductivity due to the potassium ion only (using the transference number data of Kerkhoff)

Dashed line: self diffusion coefficient calculated from the conductivity due to potassium ion only (using the extrapolated transference number data of Kerkhoff)

Open circles: self diffusion coefficients measured by radioactive tracer (present work)

Dark circles: self diffusion coefficients measured by radioactive tracer (Witt)

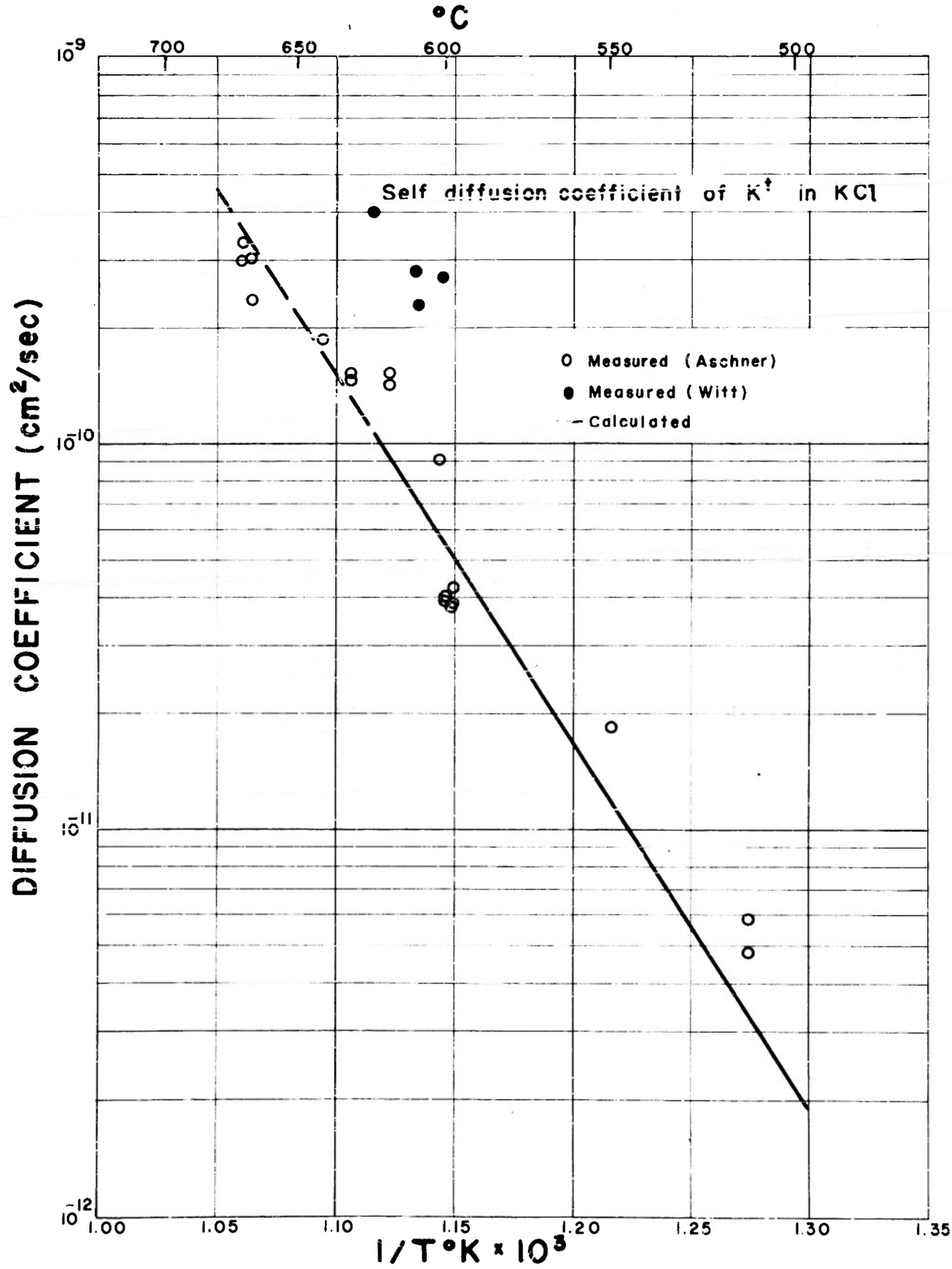
°C
700
650
600
550
500
Self diffusion coefficient of K⁺ in KCl
O Measured (Aschner)
● Measured (Witt)
— Calculated
DIFFUSION COEFFICIENT (cm²/sec)
10⁻⁹
10⁻¹⁰
10⁻¹¹
10⁻¹²
1.00
1.05
1.10
1.15
1.20
1.25
1.30
1.35
1/T°K × 10³

TECHNICAL REPORTS DISTRIBUTION LIST

University of Illinois
Contract N6onr-07129
NR 017-412

A. Government Distribution

Department of Defense

Research and Development Board
Pentagon Building
Washington 25, D. C. (2 copies)

Department of the Navy

Chief of Naval Research
Office of Naval Research
Washington 25, D. C.
Attn: Physics Branch (2 copies)

Director, Naval Research Laboratory
Washington 20, D. C.
Attn: Technical Information Officer (9 copies)

ONR, Branch Offices

Commanding Officer
U. S. Navy Office of Naval Research
Branch Office
346 Broadway
New York 13, New York (1 copy)

Commanding Officer
Office of Naval Research
Branch Office
The John Crear Library Building
Tenth Floor, 86 E. Randolph Street
Chicago 1, Illinois
Telephone: Central 6-4288

Commanding Officer
U. S. Navy Office of Naval Research
Branch Office
801 Donahue Street
San Francisco 24, California (1 copy)

Commanding Officer
U. S. Navy Office of Naval Research
Branch Office
1030 East Green Street
Pasadena 1, California (1 copy)

Government Distribution List continued

Office of Assistant Naval Attache for Research
Navy No. 100, Fleet Post Office
New York, New York (2 copies)

Director
Naval Research Laboratory
Washington 20, D. C.
Attn: Code 2021 (1 copy)

Chief of Bureau of Aeronautics
Navy Department
Washington 25, D. C. (1 copy)

Chief of Bureau of Ordnance
Navy Department
Washington 25, D. C.
Attn: Code REA (1 copy)

Chief of Bureau of Ships
Navy Department
Washington 25, D. C.
Attn: Code 330 (1 copy)

Department of the Air Forces

Army Air Forces
War Department
Washington 25, D. C.
Attn: A.E./A.S. -2 Collection Branch (1 copy)

Department of the Army

Chief, Engineering and Technical Division
Office of the Chief Signal Officer
SIGTM-5 - The Pentagon
Washington 25, D. C. (1 copy)

Department of Commerce

Director
National Bureau of Standards
Washington 25, D. C. (1 copy)

National Research Council
Division of Physical Sciences
2101 Constitution Avenue
Washington 25, D. C. (1 copy)

Dr. L. R. Maxwell
Naval Ordnance Laboratory
Silver Spring, Maryland (1 copy)

Government Distribution List continued

Los Alamos Scientific Laboratory
Los Alamos, New Mexico
Attn: Dr. Calvin Potts (1 copy)

B. Non-Government Distribution

Brown University
Department of Physics
Providence, Rhode Island
Attn: H. E. Farnsworth (1 copy)

Case School of Applied Science
Department of Physics
Cleveland, Ohio
Attn: E. C. Crittenden, Jr. (1 copy)

Cornell University
Department of Physics
Ithaca, New York
Attn: Lloyd P. Smith (1 copy)

Director, Research Laboratory of Electronics
Massachusetts Institute of Technology
Cambridge 39, Massachusetts
Attn: J. A. Stratton (1 copy)

Director of Laboratory for Insulation Research
Massachusetts Institute of Technology
Cambridge 39, Massachusetts
Attn: A. Von Hipple (1 copy)

Oregon State College
Department of Chemistry
Corvallis, Oregon
Attn: Dr. A. B. Scott (1 copy)

California Institute of Technology
Division of Chemistry and Chemical Engineering
Pasadena, California
Attn: Dr. L. Pauling (1 copy)

University of California
Department of Physics
Berkeley, California
Attn: Leonard B. Loeb (1 copy)

Non-Government Distribution List continued

University of Pennsylvania
Department of Physics
Philadelphia Pennsylvania
Attn: W. E. Stephens (1 copy)
H. B. Callen (1 copy)
F. C. Hix (1 copy)

Washington State College
Department of Physics
Pullman, Washington
Attn: P. W. Anderson (1 copy)

Smith College
Department of Chemistry
Northhampton, Massachusetts
Attn: Dr. G. S. Dunham (1 copy)

Dr. E. Billig, Head
General Physics Department
Associated Electrical Industries, Ltd.
Aldermaston, Berkshire, England
Via: Office of the Assistant Naval
Attache for Research
Navy No. 100
Fleet Post Office
New York 4, New York (1 copy)

Ohio State University
Department of Physics
Columbus 10, Ohio
Attn: Dr. P. M. Harris (1 copy)

Dr. R. J. Maurer
Department of Physics
University of Illinois
Urbana, Illinois (1 copy)

Dr. Frederick Seitz
Department of Physics
University of Illinois
Urbana, Illinois (1 copy)

Dr. Karl Lark-Horovitz
Purdue University
Department of Physics
Lafayette, Indiana (1 copy)

Dr. L. W. McKeehan
Yale University
Sloane Physics Laboratory
New Haven, Connecticut (1 copy)

Non-Government Distribution List continued

Dr. R. C. Hermann
8621 Georgia Avenue
Applied Physics Laboratory
The Johns Hopkins University
Silver Spring, Maryland

Note: In those cases where an ONR Resident Representative has cognizance of the contract, one copy of the technical report should be sent to the Representative.